14. Nishimura, H., and T. Honjo. 2001. PD-1: an inhibitory immunoreceptor involved in peripheral tolerance. *Trends Immunol. 22:265.*
15. Okazaki, T., Y. Iwai, and T. Honjo. 2002. New regulatory co-receptors: inducible co-stimulator and PD-1. *Curr. Opin. Immunol. 14:779.*
16. Salama, A. D., T. Chitnis, J. Imitola, M. J. Ansari, H. Akiba, F. Tushima, M. Azuma, H. Yagita, M. H. Sayegh, and S. J. Khoury. 2003. Critical role of the programmed death-1 (PD-1) pathway in regulation of experimental autoimmune encephalomyelitis. *J. Exp. Med. 198:71.*
17. Liang, S. C., Y. E. Latchman, J. E. Buhlmann, M. F. Tomczak, B. H. Horwitz, G. J. Freeman, and A. H. Sharpe. 2003. Regulation of PD-1, PD-L1, and PD-L2 expression during normal and autoimmune responses. *Eur. J. Immunol. 33:2706.*
18. Ansari, M. J., A. D. Salama, T. Chitnis, R. N. Smith, H. Yagita, H. Akiba, T. Yamazaki, M. Azuma, H. Iwai, S. J. Khoury, et al. 2003. The programmed death-1 (PD-1) pathway regulates autoimmune diabetes in nonobese diabetic (NOD) mice. *J. Exp. Med. 198:63.*
19. Fairchild, P. J., F. A. Brook, R. L. Gardner, L. Graca, V. Strong, Y. Tone, M. Tone, K. F. Nolan, and H. Waldmann. 2000. Directed differentiation of dendritic cells from mouse embryonic stem cells. *Curr. Biol. 10:1515.*
20. Matsuyoshi, H., S. Senju, S. Hirata, Y. Yoshitake, Y. Uemura, and Y. Nishimura. 2004. Enhanced priming of antigen-specific CTLs in vivo by embryonic stem cell-derived dendritic cells expressing chemokine along with antigenic protein: application to antitumor vaccination. *J. Immunol. 172:776.*
21. Fairchild, P. J., K. F. Nolan, S. Cartland, L. Graca, and H. Waldmann. 2003. Stable lines of genetically modified dendritic cells from mouse embryonic stem cells. *Transplantation 76:606.*
22. Cheng, P., Y. Nefedova, L. Miele, B. A. Osborne, and D. Gabrilovich. 2003. Notch signaling is necessary but not sufficient for differentiation of dendritic cells. *Blood 102:3980.*
23. Mendel, I., N. Kerlero de Rosbo, and A. Ben-Nun. 1995. A myelin oligodendrocyte glycoprotein peptide induces typical chronic experimental autoimmune encephalomyelitis in H-2^b mice: fine specificity and T cell receptor Vβ expression of encephalitogenic T cells. *Eur. J. Immunol. 25:1951.*
24. Greer, J. M., R. A. Sobel, A. Sette, S. Southwood, M. B. Lees, and V. K. Kuchroo. 1996. Immunogenic and encephalitogenic epitope clusters of myelin proteolipid protein. *J. Immunol. 156:371.*
25. Zamvil, S. S., D. J. Mitchell, M. B. Powell, K. Sakai, J. B. Rothbard, and L. Steinman. 1988. Multiple discrete encephalitogenic epitopes of the autoantigen myelin basic protein include a determinant for I-E class II-restricted T cells. *J. Exp. Med. 168:1181.*
26. Senju, S., K. Iyama, H. Kudo, S. Aizawa, and Y. Nishimura. 2000. Immunocytochemical analyses and targeted gene disruption of GTPBP1. *Mol. Cell. Biol. 20:6195.*
27. Fujii, S., Y. Uemura, L. K. Iwai, M. Ando, S. Senju, and Y. Nishimura. 2001. Establishment of an expression cloning system for $CD4^+$ T cell epitopes. *Biochem. Biophys. Res. Commun. 284:1140.*
28. Uemura, Y., S. Senju, K. Maenaka, L. K. Iwai, S. Fujii, H. Tabata, H. Tsukamoto, S. Hirata, Y. Z. Chen, and Y. Nishimura. 2003. Systematic analysis of the combinatorial nature of epitopes recognized by TCR leads to identification of mimicry epitopes for glutamic acid decarboxylase 65-specific TCRs. *J. Immunol. 170:947.*
29. Weir, C. R., K. Nicolson, and B. T. Backstrom. 2002. Experimental autoimmune encephalomyelitis induction in naive mice by dendritic cells presenting a self-peptide. *Immunol. Cell Biol. 80:14.*
30. Legge, K. L., R. K. Gregg, R. Maldonado-Lopez, L. Li, J. C. Caprio, M. Moser, and H. Zaghouani. 2002. On the role of dendritic cells in peripheral T cell tolerance and modulation of autoimmunity. *J. Exp. Med. 196:217.*
31. Bonham, C. A., L. Lu, R. A. Banas, P. Fontes, A. S. Rao, T. E. Starzl, A. Zeevi, and A. W. Thomson. 1996. TGF-β1 pretreatment impairs the allostimulatory function of human bone marrow-derived antigen-presenting cells for both naive and primed T cells. *Transpl. Immunol. 4:186.*
32. Lutz, M. B., R. M. Suri, M. Niimi, A. L. Ogilvie, N. A. Kukutsch, S. Rossner, G. Schuler, and J. M. Austyn. 2000. Immature dendritic cells generated with low doses of GM-CSF in the absence of IL-4 are maturation resistant and prolong allograft survival in vivo. *Eur. J. Immunol. 30:1813.*
33. Steinbrink, K., M. Wolfl, H. Jonuleit, J. Knop, and A. H. Enk. 1997. Induction of tolerance by IL-10-treated dendritic cells. *J. Immunol. 159:4772.*
34. Menges, M., S. Rossner, C. Voigtlander, H. Schindler, N. A. Kukutsch, C. Bogdan, K. Erb, G. Schuler, and M. B. Lutz. 2002. Repetitive injections of dendritic cells matured with tumor necrosis factor-α induce antigen-specific protection of mice from autoimmunity. *J. Exp. Med. 195:15.*
35. Sato, K., N. Yamashita, M. Baba, and T. Matsuyama. 2003. Regulatory dendritic cells protect mice from murine acute graft-versus-host disease and leukemia relapse. *Immunity 18:367.*
36. Sato, K., N. Yamashita, M. Baba, and T. Matsuyama. 2003. Modified myeloid dendritic cells act as regulatory dendritic cells to induce anergic and regulatory T cells. *Blood 101:3581.*
37. Dhodapkar, M. V., R. M. Steinman, J. Krasovsky, C. Munz, and N. Bhardwaj. 2001. Antigen-specific inhibition of effector T cell function in humans after injection of immature dendritic cells. *J. Exp. Med. 193:233.*
38. Takayama, T., Y. Nishioka, L. Lu, M. T. Lotze, H. Tahara, and A. W. Thomson. 1998. Retroviral delivery of viral interleukin-10 into myeloid dendritic cells markedly inhibits their allostimulatory activity and promotes the induction of T-cell hyporesponsiveness. *Transplantation 66:1567.*
39. Lu, L., A. Gambotto, W. C. Lee, S. Qian, C. A. Bonham, P. D. Robbins, and A. W. Thomson. 1999. Adenoviral delivery of CTLA4Ig into myeloid dendritic cells promotes their in vitro tolerogenicity and survival in allogeneic recipients. *Gene Ther. 6:554.*
40. Min, W. P., R. Gorczynski, X. Y. Huang, M. Kushida, P. Kim, M. Obataki, J. Lei, R. M. Suri, and M. S. Cattral. 2000. Dendritic cells genetically engineered to express Fas ligand induce donor-specific hyporesponsiveness and prolong allograft survival. *J. Immunol. 164:161.*
41. Terness, P., T. M. Bauer, L. Rose, C. Dufter, A. Watzlik, H. Simon, and G. Opelz. 2002. Inhibition of allogeneic T cell proliferation by indoleamine 2,3-dioxygenase-expressing dendritic cells: mediation of suppression by tryptophan metabolites. *J. Exp. Med. 196:447.*
42. Liu, Z., X. Xu, H. C. Hsu, A. Tousson, P. A. Yang, Q. Wu, C. Liu, S. Yu, H. G. Zhang, and J. D. Mountz. 2003. CII-DC-AdTRAIL cell gene therapy inhibits infiltration of CII-reactive T cells and CII-induced arthritis. *J. Clin. Invest. 112:1332.*
43. Morita, Y., J. Yang, R. Gupta, K. Shimizu, E. A. Shelden, J. Endres, J. J. Mule, K. T. McDonagh, and D. A. Fox. 2001. Dendritic cells genetically engineered to express IL-4 inhibit murine collagen-induced arthritis. *J. Clin. Invest. 107:1275.*
44. Giovarelli, M., P. Musiani, G. Garotta, R. Ebner, E. Di Carlo, Y. Kim, P. Cappello, L. Rigamonti, P. Bernabei, F. Novelli, et al. 1999. A "stealth effect": adenocarcinoma cells engineered to express TRAIL elude tumor-specific and allogeneic T cell reactions. *J. Immunol. 163:4886.*
45. Brown, J. A., D. M. Dorfman, F. R. Ma, E. L. Sullivan, O. Munoz, C. R. Wood, E. A. Greenfield, and G. J. Freeman. 2003. Blockade of programmed death-1 ligands on dendritic cells enhances T cell activation and cytokine production. *J. Immunol. 170:1257.*
46. Carter, L., L. A. Fouser, J. Jussif, L. Fitz, B. Deng, C. R. Wood, M. Collins, T. Honjo, G. J. Freeman, and B. M. Carreno. 2002. PD-1:PD-L inhibitory pathway affects both $CD4^+$ and $CD8^+$ T cells and is overcome by IL-2. *Eur. J. Immunol. 32:634.*
47. Selenko-Gebauer, N., O. Majdic, A. Szekeres, G. Hofler, E. Guthann, U. Korthauer, G. Zlabinger, P. Steinberger, W. F. Pickl, H. Stockinger, et al. 2003. B7-H1 (programmed death-1 ligand) on dendritic cells is involved in the induction and maintenance of T cell anergy. *J. Immunol. 170:3637.*

THE JOURNAL OF BIOLOGICAL CHEMISTRY
Vol. 279, No. 46, Issue of November 12, pp. 48457–48465, 2004
Printed in U.S.A.

B-Raf Contributes to Sustained Extracellular Signal-regulated Kinase Activation Associated with Interleukin-2 Production Stimulated through the T Cell Receptor*

Received for publication, March 19, 2004, and in revised form, August 27, 2004
Published, JBC Papers in Press, August 31, 2004, DOI 10.1074/jbc.M403087200

Hirotake Tsukamoto, Atsushi Irie, and Yasuharu Nishimura‡

From the Department of Immunogenetics, Graduate School of Medical Sciences, Kumamoto University, Honjo 1-1-1, Kumamoto 860-8556, Japan

A T cell receptor (TCR) recognizes and responds to an antigenic peptide in the context of major histocompatibility complex-encoded molecules. This provokes T cells to produce interleukin-2 (IL-2) through extracellular signal-regulated kinase (ERK) activation. We investigated the roles of B-Raf in TCR-mediated IL-2 production coupled with ERK activation in the Jurkat human T cell line. We found that TCR cross-linking could induce up-regulation of both B-Raf and Raf-1 activities, but Raf-1 activity was decreased rapidly. On the other hand, TCR-stimulated kinase activity of B-Raf was sustained. Expression of a dominant-negative mutant of B-Raf abrogated sustained but not transient TCR-mediated MEK/ERK activation. The inhibition of sustained ERK activation by either expression of a dominant-negative B-Raf or treatment with a MEK inhibitor resulted in a decrease of the TCR-stimulated nuclear factor of activated T cells (NFAT) activity and IL-2 production. Collectively, our data provide the first direct evidence that B-Raf is a positive regulator of TCR-mediated sustained ERK activation, which is required for NFAT activation and the full production of IL-2.

T cells recognize self or non-self peptides in the context of major histocompatibility complex (MHC)[1]-encoded molecules via T cell receptors (TCRs), and the signals are then transduced into the nucleus. These signals determine the fate of T cells and induce cytokine production, cytolytic activity, survival, apoptosis, and proliferation (1). Within seconds of MHC-peptide engagement, TCR components initiate phosphorylation cascades that trigger multiple branching signaling pathways. One well studied key switch is the activation signal of extracellular signal-regulated kinase 1/2 (ERK1/2), which is mediated by the small GTP-binding proteins, Ras (2, 3) and Rap1 (4, 5). Current models suggest that TCR stimulation with the agonistic peptide-MHC complex activates the conversion of Ras from the GDP- to GTP-bound form (2, 6). Activated Ras subsequently recruits the serine/threonine kinase Raf-1 to the plasma membrane, resulting in its activation. Activated Raf-1 then activates ERK kinase (MEK), which directly phosphorylates tyrosine and threonine residues (TEY motif) on ERK1/2 to activate them (6). These signals combine to activate multiple transcription factors, including nuclear factor of activated T cells (NFAT), NF-κB, and activating protein-1 (AP-1), all of which contribute toward the production of IL-2 (7–9).

ERK1/2 are involved in a diverse array of cellular functions including cell growth and apoptosis of T cells (10–12). In ERK1-deficient mice, the thymocyte differentiation from $CD4^+CD8^+$ double positive to the $CD4^+/CD8^+$ single positive stage is impaired; thus, ERK activation by TCR ligation plays important roles in T cell development (13). Experiments using pharmacological inhibitors of MEK and dominant negative MEK also provided evidence that ERK1/2 are critical for thymocyte differentiation (11, 14) and for induction of TCR-mediated mitogenic signals and IL-2 production in mature T cells (7, 15). Hence, it is important to understand how the strength and duration of ERK activity is regulated in TCR-mediated activation and fate decisions of T cells.

The functions of ERK signaling are regulated by its upstream elements, in particular by members of the Raf family, in various cell types, and three Raf isoforms, Raf-1, A-Raf, and B-Raf, are expressed in mammalian cells (16, 17). Whereas Raf-1 is ubiquitously expressed, B-Raf shows a more restricted expression pattern (18, 19). Mice deficient in the different Raf isoforms exhibit different developmental defects, suggesting the nonredundant function(s) of each Raf isoform (20). A different phenotype of each Raf-deficient mouse is expected to be due, at least in part, to their distinct expression pattern. It was reported that B-Raf exhibits a much more basal kinase activity and a higher affinity toward MEK than does Raf-1 *in vitro* (21). Despite these differences, the specific function(s) *in vivo*, if any, of each Raf isoform is poorly understood. B-Raf was reported to be one component of the receptor-mediated MEK/ERK activation pathway in fibroblasts, B cell lines, and PC12 cells (21–26). Moreover, B-Raf expression in T cells is controversial; in this study, we detected B-Raf protein in Jurkat cells and primary human T cells, whereas others did not (4).

Although Raf-1 is a well characterized effector molecule for ERK activation in the TCR-mediated signaling cascade and IL-2 production in T cells (27), much less attention has been directed to the roles of B-Raf in T cells. We now report that interaction of B-Raf with MEK and B-Raf activity are induced in a TCR stimulation-dependent manner in Jurkat cells. Our data suggest that MEK/ERK activity are selectively regulated through the Ras/B-Raf signaling pathway and that the sustained B-Raf/MEK/ERK activation is indispensable for the

* This work was supported in part by Grants-in-Aid 12051203, 14370115, and 15510165 from the Ministry of Education, Science, Technology, Sports, and Culture, Japan. The costs of publication of this article were defrayed in part by the payment of page charges. This article must therefore be hereby marked "*advertisement*" in accordance with 18 U.S.C. Section 1734 solely to indicate this fact.

‡ To whom correspondence should be addressed: Dept. of Immunogenetics, Graduate School of Medical Sciences, Kumamoto University, Honjo 1-1-1, Kumamoto 860-8556, Japan. Tel.: 81-96-373-5310; Fax: 81-96-373-5314; E-mail: mxnishim@gpo.kumamoto-u.ac.jp.

[1] The abbreviations used are: MHC, major histocompatibility complex; AP-1, activating protein-1; ERK, extracellular signal-regulated kinase; GST, glutathione *S*-transferase; HA, hemagglutinin; IL-2, interleukin-2; MEK, mitogen-activated protein kinase/ERK kinase; NFAT, nuclear factor of activated T cells; TCR, T cell receptor; GFP, green fluorescent protein.

translocation of NFAT into the nucleus and for the production of IL-2.

EXPERIMENTAL PROCEDURES

Cell Preparations and Reagents—Jurkat cell clone, E6-1 from the American Type Culture Collection, and Jurkat cells expressing simian virus 40 large T antigen (TAg-Jurkat) (28) were maintained in RPMI 1640 medium (RPMI) supplemented with 10% fetal calf serum, 2 mM L-glutamine, and penicillin/streptomycin (100 units/ml and 100 μg/ml, respectively). Jurkat cells stably expressing a wild-type or a dominant negative form of B-Raf were established and maintained in RPMI plus 10% fetal calf serum with 2 mg/ml G418. The human $CD4^+$ T cell clone, YN 5–32 and peripheral blood mononuclear cells were prepared as described (29, 30). For transient and stable transfection, 2×10^7 Jurkat cells were resuspended in 500 μl of cytomix (31) with the appropriate cDNAs. The amount of plasmid DNA was held at 40 μg constant by the addition of the pcDNA3 vector control. Cells were electroporated in 310 V at a capacitance of 960 microfarads. Transfectants were analyzed for CD3 and CD28 expression using flow cytometry (BD Biosciences). Anti-CD3 (clone UCHT-1) antibody, anti-CD28 (clone L923) antibody, and rabbit polyclonal anti-GFP antibody were purchased from Pharmingen. Anti-mouse IgG (Fab-specific) antibody was from Sigma. Mouse monoclonal anti-NFAT1 and anti-NFAT2 antibodies and rabbit polyclonal antibodies specific to Raf-1, B-Raf, MEK-1, c-Fos, and Lamin B were purchased from Santa Cruz Biotechnology, Inc. (Santa Cruz, CA). Polyclonal antibodies specific to MEK, phospho-ERK, phospho-p38, and phospho-MEK and a MEK inhibitor, U0126, were purchased from New England Biolabs (Beverly, MA). Mouse monoclonal anti-hemagglutinin (HA) antibody was from Covance (Berkeley, CA). Cy3-labeled anti-rabbit Ig antibody, horseradish peroxidase-conjugated rabbit anti-mouse IgG, and donkey anti-rabbit IgG were from Amersham Biosciences. Anti-human IL-2 antibodies were from R & D Systems (Minneapolis, MN). Recombinant glutathione *S*-transferase (GST)-MEK was prepared as reported (32).

The pcDNA3 expression vectors with HA-tagged wild-type and dominant negative mutant B-Raf cDNAs were provided by Dr. K. L. Guan (33). The RasN17 expression vector was a gift from Dr. T. Kinashi (5). The luciferase reporter construct for IL-2 promoter and AP-1 binding site were kindly provided by Dr. V. A. Boussiotis (34) and Dr. R. M. Niles (35), respectively. The expression vector for GST-MEK was a gift from Dr. Y. Takai (32). NFAT-green fluorescence protein (GFP) reporter construct, consisting of three tandem NFAT-binding sites followed by a gene encoding GFP, was provided by Dr. T. Saito (36).

Cell Stimulation and Inhibitor Treatment—In experiments for stimulation with soluble anti-CD3 antibody for cross-linking, Jurkat cells were incubated on ice for 20 min and then incubated with anti-CD3 antibody (0.25 μg/ml) for 10 min followed by the addition of anti-mouse IgG antibody (1 μg/ml) for 5 min. After the indicated times of incubation at 37 °C, cells were harvested and lysed with lysis buffer (see below). For the analysis of promoter activity and IL-2 production, Jurkat cells (1×10^6/well) were stimulated with immobilized anti-CD3 and CD28 antibodies (5 and 10 μg/ml, respectively). For experiments with inhibitor treatment, cells were preincubated for 30 min with the MEK inhibitor U0126 or Me_2SO as a control. In the time course analyses of the effect of ERK activation on IL-2 production by the treatment with U0126, medium containing U0126 or Me_2SO was added at the indicated time points.

Western Blotting, Immunoprecipitation, and in Vitro Kinase Assay—After the indicated times of stimulation, the Jurkat cells were recovered and lysed with lysis buffer (1% Nonidet P-40, 150 mM NaCl, 50 mM Tris, pH 7.4, 1 mM EDTA, 0.25% sodium deoxycholate, a protease inhibitor tablet (Roche Applied Science)). SDS-PAGE, Western blotting, and immunoprecipitations from the cell lysates were carried out as described (30). Raf-1 and B-Raf were immunoprecipitated from cell lysates of T cells with the anti-Raf-1 and the anti-B-Raf antibodies, respectively, as described above. The immunoprecipitates were resuspended in 25 mM HEPES (pH 7.5), 10 mM $MgCl_2$, 10 mM β-glycerophosphate, 1 mM dithiothreitol, 10 μCi of [γ-^{32}P]ATP (Amersham Biosciences), and 0.8 μg of recombinant GST-MEK protein. Reaction mixtures were incubated at 32 °C for 20 min, and then the reactions were terminated by adding 5× SDS sample buffer, separated on 7% SDS-PAGE under the reducing condition, transferred to nitrocellulose membrane, and exposed to x-ray film. Relative amounts of MEK or ERK phosphorylation were calculated based on the ratio of the intensities of phospho-MEK or phospho-ERK bands to those of the whole MEK or ERK bands in whole cell lysates at each time point. Signal intensities of the bands were quantified by densitometric analysis using NIH Image 6.2 software. Nuclear extracts were prepared from B-Raf mutant- or mock-transfected TAg Jurkat cells for nuclear translocation analysis of NFAT using nuclear/cytosol fractionation kits (BioVision).

Flow Cytometric Analysis and Cytokine Measurement—For the NFAT-GFP reporter assay, the TAg-Jurkat cells expressing B-Raf AA or mock vector were transfected with NFAT-GFP reporter construct and stimulated for 9 h with immobilized anti-CD3 and anti-CD28 antibodies. The expression of GFP was analyzed with a flow cytometer and CellQuest software (BD Biosciences). For intracellular staining, cells were fixed and permeabilized with IntraPrep (Immunotech, Marseille, France) and then stained with appropriate fluorescence-labeled antibodies. IL-2 concentrations in supernatants of T cell culture after 48 h of stimulation were measured in an enzyme-linked immunosorbent assay using anti-human IL-2 antibodies.

Reverse Transcription-PCR—Total RNA extraction and first-strand cDNA synthesis from T cells were done as described (37). The cDNA was subjected to PCR amplification using a set of primers specific for human *B-Raf*: 5′-ACAACAGTTATTGGAATCTCTGG-3′ and 5′-AAATGCTAAGGTGAAAAACG-3′.

Luciferase Assay—Reporter constructs were transfected into the Jurkat cells expressing wild-type or mutant B-Raf. A β-galactosidase expression plasmid was co-transfected to normalize the variations in transfection efficiency. After 12 h of transfection, cells were harvested and stimulated. Luciferase assay was carried out according to the protocol in the Pica Gene kit (Toyo Ink, Tokyo, Japan). β-Galactosidase expression was assessed using the Luminescent β-galactosidase detection kit II (Clontech) according to the manufacturer's instructions.

RESULTS

Expression of B-Raf Proteins in Both Human and Mouse T Cells—We investigated the expression of B-Raf in human and mouse T cells using Western blotting (Fig. 1*A*). Rat PC12 cells, as a positive control gave a 95-kDa band corresponding to B-Raf (*lane 1*), whereas B-Raf expression was negligible in NIH3T3 cells, as reported (*lane 2*) (38). B-Raf was detected in a human $CD4^+$ T cell clone, YN5–32 (*lane 3*) (29, 30), a human T cell line, Jurkat (*lane 4*), and mouse $CD4^+$ T cells isolated from spleens (*lanes 5*). Furthermore, the expression of human B-Raf mRNA was assessed by reverse transcription-PCR using RNAs isolated from the YN5–32 T cell clone and from Jurkat T cells (data not shown). Intracellular staining and flow cytometric analysis also confirmed the B-Raf expression in human CD3-positive peripheral T cells (Fig. 1*B*) and mouse TCR-β chain-positive splenic T cells (Fig. 1*B*, *b*). Taken together, we conclude that B-Raf is expressed in both human and mouse T cells, allowing us to examine B-Raf functions in TCR-mediated T cell activation.

TCR Ligation Induces Both Raf-1 and B-Raf Activation—Cross-linking of TCRs with soluble anti-CD3 antibody, which mimics the engagement of TCR with the agonistic peptide-MHC complex, induced ERK and MEK phosphorylation within 1 min, reaching a maximal level at ~1–3 min in Jurkat cells (Fig. 2*A*). The ERK/MEK phosphorylations displayed similar kinetics and were prolonged for up to 60 min. Next, we performed *in vitro* kinase assays for Raf-1 and B-Raf to estimate the strength and kinetics of their kinase activities. Consistent with the previous report (27), Raf-1 was activated at 3 min after TCR ligation and became inactive within 20 min (Fig. 2*B*). In contrast to the kinetics of Raf-1 activity, there was slight but detectable B-Raf activity even under the basal condition, and B-Raf showed a pronounced increase of its kinase activity at 3 min after TCR stimulation. B-Raf kinase activity was gradually decreased but did last for up to 60 min (Fig. 2*B*). Raf-1 was inactivated after 20 min of TCR ligation; nevertheless, apparent MEK/ERK activation was still sustained up to 60 min (Fig. 2*A*). Intriguingly, the kinetics of TCR-mediated B-Raf activation rather than that of Raf-1 activation was similar to that of MEK/ERK activation. The addition of co-stimulation with an anti-CD28 antibody treatment slightly enhanced the B-Raf activity over time compared with that stimulated with an anti-CD3 antibody alone (Fig. 2*C*).

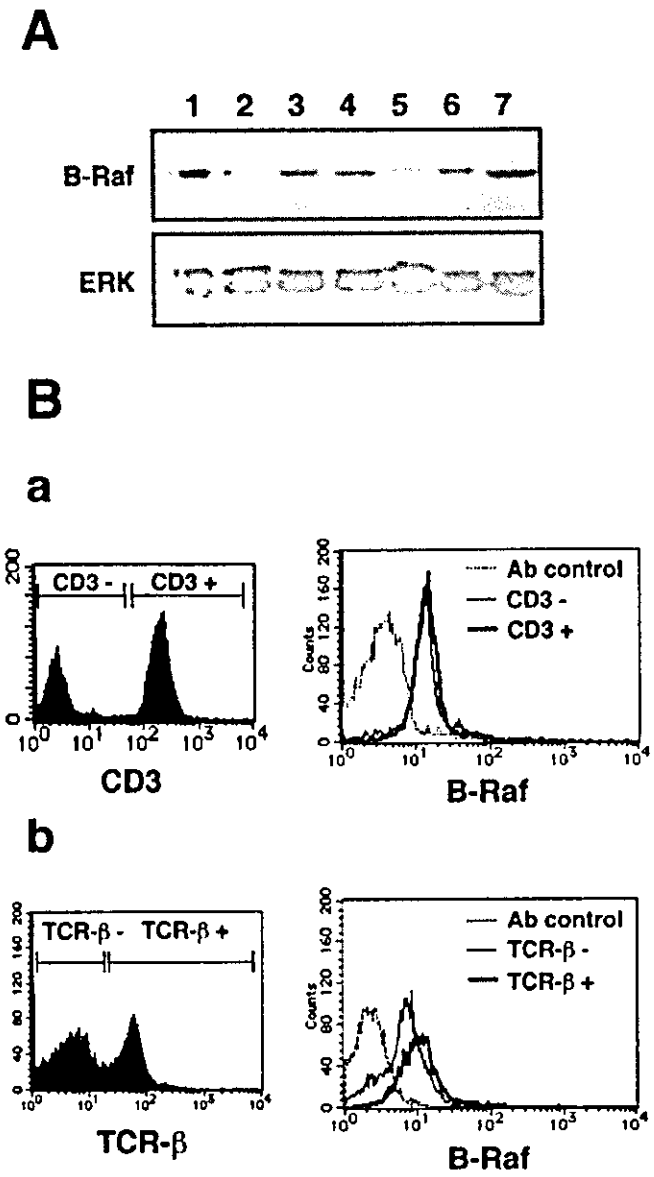

FIG. 1. **B-Raf is expressed in both human and mouse T cells.** *A*, Western blotting analysis using an anti-B-Raf antibody (*top panel*). *Lane 1*, PC12 cells; *lane 2*, NIH3T3 cells; *lane 3*, human $CD4^+$ T cell clone, YN5–32; *lane 4*, Jurkat cells; *lane 5*, mouse $CD4^+$ T cells isolated from spleen; *lane 6*, HeLa cells; *lane 7*, HeLa cells transfected with B-Raf. ERK blotting indicates comparable protein loading (*bottom panel*). *B*, flow cytometric analyses of B-Raf expression. Human peripheral blood mononuclear cells were stained with an anti-CD3 antibody (*a*) and murine spleen cells were stained with anti-mouse TCR-β chain antibody (*b*) (*left panels*). The CD3 or TCR-β chain negative and positive cell populations were gated, and intracellular B-Raf staining was carried out (*right panels*). An irrelevant rabbit polyclonal antibody was used as negative control for staining. *Ab*, antibody.

Physiological association between Raf family kinases and MEK is necessary for MEK/ERK activation (39); hence, we asked if B-Raf can interact with MEK in T cells in response to TCR stimulation using co-immunoprecipitation methods. For this purpose, wild-type B-Raf tagged with HA was expressed in Jurkat cells and was immunoprecipitated with an anti-HA antibody. The specific association between HA-B-Raf and MEK was achieved at a maximal level at 3 min after TCR ligation, and this interaction lasted for up to 60 min with a slight decrease (Fig. 2*D*). The intrinsic interaction between B-Raf and MEK was also evaluated by reciprocal immunoprecipitation experiments using an anti-MEK antibody to detect endogenous B-Raf protein. As shown in Fig. 2*E*, endogenous B-Raf protein was not detected in immunoprecipitates with the anti-MEK antibody in unstimulated Jurkat cells. Consistent with Fig. 2*D*, intrinsic B-Raf·MEK complex formation was strongly induced at 3 min after TCR ligation, and then it decreased gradually but remained above the basal level up to 60 min after TCR stimulation *in vivo* (Fig. 2*E*). The kinetics of B-Raf/MEK interaction paralleled those of B-Raf activation (Fig. 2*B*). These results strongly suggested that B-Raf was involved in MEK/ERK activation stimulated with TCR ligation, especially in the late phase after Raf-1 had become inactive (Fig. 2*B*).

TCR-mediated B-Raf Activation Is Partly Dependent on Ras Activity—Previous studies reported that B-Raf activation in fibroblasts was dependent on Ras activation (40, 41). In other cases, Ras activity was not essential for B-Raf activation in PC12 cells (23, 38). In T cells, to determine whether Ras activity is required for the B-Raf activation, TCR-mediated B-Raf activity was measured in TAg-Jurkat expressing the dominant negative Ras mutant RasN17. The RasN17 interfered with endogenous Ras, Raf-1, and MEK/ERK activation until at least 60 min after TCR stimulation (data not shown) (2). As shown in Fig. 3, TCR engagement resulted in a robust activation of B-Raf after stimulation in mock-transfected Jurkat cells. In contrast, RasN17-transfected cells showed decreased B-Raf activation as compared with that observed in the control cells at 3 min after TCR stimulation (75% reduction). Similar inhibitory effects was observed at any given time points. These results indicated that TCR-mediated B-Raf activation is, at least in part, regulated by Ras activation *in vivo*.

B-Raf Contributes to Sustained MEK/ERK Activation—Within the activation segment of B-Raf, there are two sites, Thr^{598} and Ser^{601}, that can be phosphorylated in response to Ras activation, and the phosphorylation status of these residues is required for the maximal kinase activity of B-Raf (33, 40). Hence, we introduced a dominant negative mutant of B-Raf (B-Raf AA), in which Thr^{598} and Ser^{601} were substituted to Ala (33), into T cells to examine the role of B-Raf in TCR-mediated MEK/ERK activation cascade. As shown in Fig. 4*A*, a Jurkat clone expressing B-Raf AA showed a similar degree of MEK/ERK activation induced by TCR cross-linking with soluble anti-CD3 antibody at 3 min after stimulation in comparison with that of mock-transfected cells. The MEK/ERK activation was effectively sustained for 60 min in the mock transfectants. On the other hand, in the Jurkat clone expressing B-Raf AA, MEK/ERK activation returned to the basal level within 30 min after TCR stimulation, and then it was no longer detected. Densitometric analyses of MEK/ERK activation revealed that the activation kinetic pattern rather than the relative magnitude of MEK/ERK activation was distinct between the mock-transfected clone and the B-Raf AA-expressing clone (Fig. 4*B*). Since TAg-Jurkat cells transiently transfected with B-Raf AA showed an essentially similar response, the possibility that these results were specific for one particular clone (AA2) was excluded (Fig. 4*C*). Moreover, these results were not due to the inhibition of Raf-1 activity by B-Raf AA, because the degree of TCR-mediated Raf-1 activation in B-Raf AA-expressing Jurkat cells was indistinguishable from that of mock-transfected Jurkat cells or cells expressing HA-tagged wild-type B-Raf (Fig. 4*D* and data not shown). In contrast to MEK/ERK activation, no significant differences in phosphorylation of another mitogen-activated protein kinase, p38, were detectable in both mock- and B-Raf AA-transfected TAg-Jurkat cells, suggesting that B-Raf AA did not influence p38 activation (Fig. 4*C*). The data indicate that B-Raf physiologically and specifically regulated prolonged MEK/ERK activation induced by TCR stimulation in Jurkat cells.

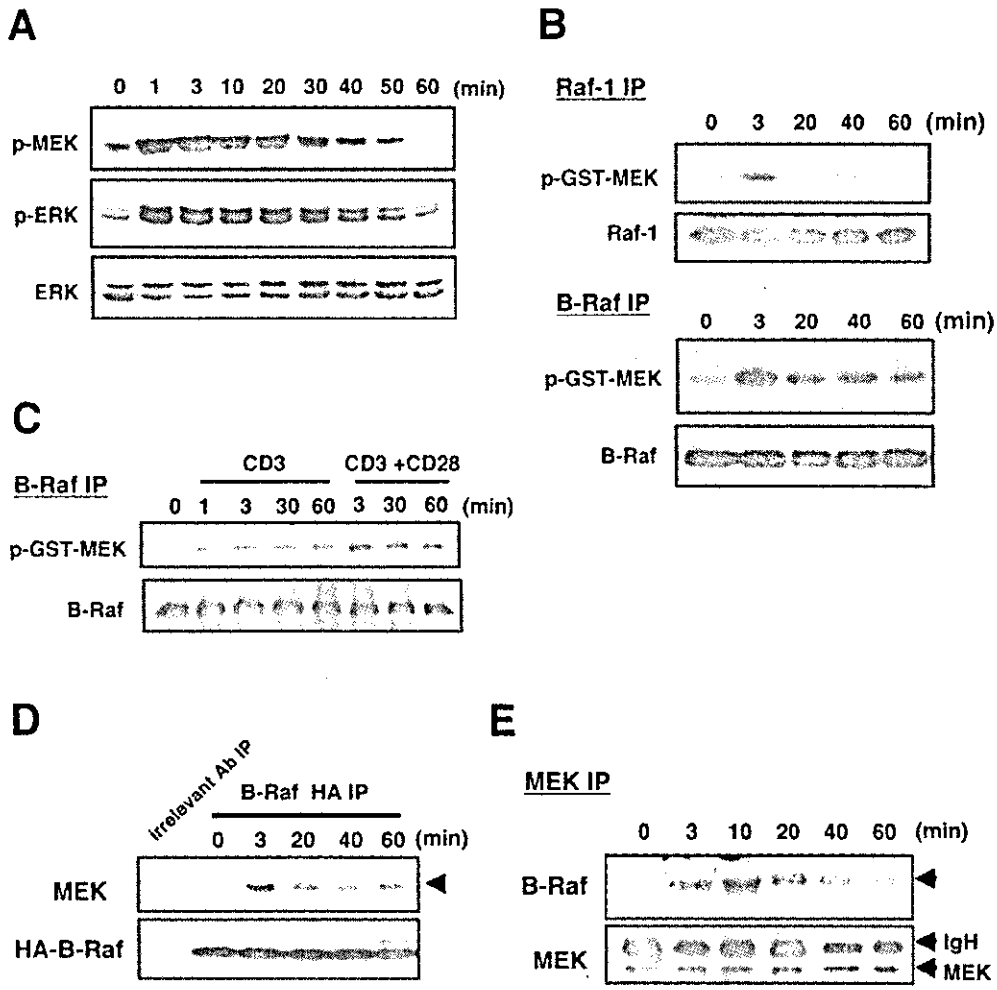

FIG. 2. **B-Raf activation and B-Raf/MEK interaction were induced in a TCR stimulation-dependent manner.** *A*, Jurkat T cells were incubated with or without (0 min) a soluble anti-CD3 antibody together with a second antibody for the indicated times. The cells were subjected to Western blotting with an anti-phospho-MEK-specific antibody (*top panel*) or an anti-phospho-ERK-specific antibody (*middle panel*). Equal protein loading was confirmed by total ERK blotting (*bottom panel*). *B*, *in vitro* kinase assays for Raf-1 and B-Raf isolated from Jurkat cells stimulated with the anti-CD3 antibody for the indicated times. Recombinant GST-MEK was used as a substrate, and incorporated ^{32}P radioactivities were visualized by autoradiography. Equal loading of each Raf protein was confirmed by blotting with either an anti-Raf-1 antibody (*upper bottom panel*) or an anti-B-Raf antibody (*lower bottom panel*). *C*, additive anti-CD28 antibody stimulation enhanced the B-Raf kinase activity. Jurkat cells were stimulated with the anti-CD3 antibody alone or the anti-CD3 together with the anti-CD28 antibodies for the indicated times, and an *in vitro* kinase assay was performed. *D*, TAg-Jurkat cells transiently expressing HA-tagged wild-type B-Raf were stimulated with cross-linking of soluble anti-CD3 antibody for the indicated times. Immunoprecipitates with an anti-HA antibody were blotted with an anti-MEK (*upper panel*) or the anti-HA antibodies (*lower panel*). The immunoprecipitates with irrelevant rabbit IgG in Jurkat cells stimulated for 3 min was used as a negative control. *E*, immunoprecipitates with an anti-MEK antibody from Jurkat cells stimulated with the anti-CD3 antibody for the indicated times were blotted with the anti-B-Raf antibody (*upper panel*). The same membrane was reprobed with the anti-MEK antibody (*lower panel*) to monitor equal protein loading. The data are representative of three reproducible experiments in all analyses. *Ab*, antibody; *IP*, immunoprecipitation.

B-Raf Activation and Subsequently Sustained ERK Activation Is Required for Full IL-2 Production—Since IL-2 production is one of the most critical events of ERK-mediated T cell activation, we first utilized the reporter assay controlled by the IL-2 promoter element to investigate the effect of B-Raf activation on IL-2 promoter activity. Whereas TCR stimulation resulted in induction of luciferase, which reflected the IL-2 promoter activity in wild-type B-Raf-transfected clone (WT30), B-Raf AA significantly attenuated the inducible IL-2 promoter activity (Fig. 5*A*). Indeed, as shown in Fig. 5*B*, TCR stimulation induced a marked increase in IL-2 production in mock-transfected Jurkat cells and in wild-type B-Raf-expressing clones (WT30 and WT34), whereas it was substantially reduced in B-Raf AA-expressing clones (AA2 and AA23).

The data described above clearly indicate that T cells expressing B-Raf AA had defects in sustained ERK activation and subsequent full IL-2 production in comparison with the control cells in response to TCR stimulation. However, whether the sustained ERK activation is directly correlated with the full IL-2 production remained to be solved. To clarify this issue, we investigated the requirement of TCR-mediated sustained ERK activation for the IL-2 production using the pharmacological MEK inhibitor U0126. As shown in Fig. 5*C*, TCR-mediated ERK activation was inhibited by U0126 at the range of 5–10 μM. In addition to ERK activation, IL-2 production provoked by stimulation with immobilized anti-CD3 and CD28 antibodies was markedly blocked by U0126 at the same range of concentrations.

We also examined the effects of B-Raf AA on the magnitude and period of ERK activation stimulated with immobilized anti-CD3 and CD28 antibodies. It must be noted that, as compared with the stimulation by cross-linking of soluble anti-CD3 antibody with the second antibody (Fig. 2*A*), stimulation with immobilized anti-CD3 and -CD28 antibodies resulted in a re-

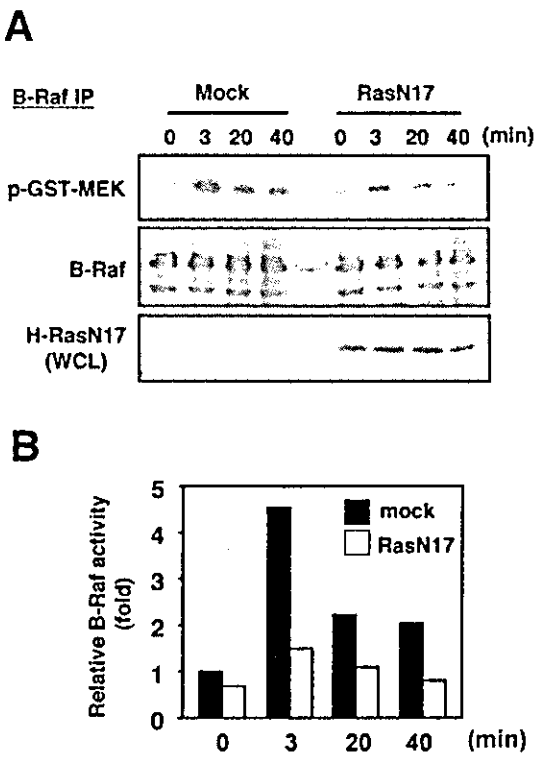

FIG. 3. **Ras-regulated B-Raf activation following TCR stimulation in Jurkat cells.** *A*, TAg-Jurkat cells were transfected with a mock vector or with the RasN17 expression vector, and then these cells were harvested and stimulated with cross-linking of soluble anti-CD3 antibody for the indicated times. Immunoprecipitates from each cell extract with an anti-B-Raf antibody were mixed with the recombinant GST-MEK as a substrate, and *in vitro* kinase reactions for B-Raf were performed. Blotting with an anti-B-Raf antibody showed equal protein loading (*middle panel*). Whole cell lysates (*WCL*) were blotted with anti-H-Ras antibody to monitor the expression of RasN17 (*lower panel*). *B*, the intensity of the GST-MEK phosphorylation by B-Raf immunoprecipitated from mock-transfected (*black bar*) or RasN17-transfected cells (*white bar*) was quantified by densitometric analysis. The relative B-Raf activity at 0 min in mock-transfected cells was assigned to be 1.0. Essentially similar results were obtained in three independent experiments. *IP*, immunoprecipitation.

tardation of ERK activation and extended ERK activation in mock-transfected cells (Fig. 5*D*). Such temporal differences in ERK activation have been reported, and the authors suggested that this phenomenon was due to the difference in TCR occupancy (42). As shown in Fig. 5*D*, in mock-transfected cells, TCR stimulation induced an accumulation of active ERK within 0.5 h, and this lasted for 6 h, whereas the sustained ERK activation over 2 or 3 h was impaired in cells expressing B-Raf AA. The data also confirmed that B-Raf was required for sustained ERK activation. Based on the results of Fig. 5*C*, 5 μM U0126 was used to determine whether the sustained ERK activation that can be suppressed by B-Raf AA, as shown in Fig. 5*D*, was required for the maximal IL-2 production. Continuous treatment of T cells with U0126 over the period of TCR stimulation abolished IL-2 production (Fig. 5*E*). Interestingly, the addition of U0126 after 2 or 4 h of TCR stimulation also reduced IL-2 production to a degree comparable with that of cells treated with U0126 from the beginning of stimulation, although the intense ERK activation was induced for up to 2 h after stimulation. The same condition in which B-Raf AA inhibited the sustained ERK activation can be reproduced by treatment of Jurkat cells with U0126 after 2 or 4 h of TCR stimulation. Therefore, not only the intense ERK activation in the early phase but also the sustained ERK activation in the late phase was necessary for maximal IL-2 production. Concomitantly, these results suggested that the defect of IL-2 production in Jurkat cells expressing B-Raf AA was due to the lack of potential to maintain the TCR-mediated sustained ERK activation although the transient ERK activation was intact.

AP-1 Activation Induced by TCR Ligation Is Not Impaired in Jurkat Cells Expressing B-Raf AA—To define more precisely the biochemical mechanisms underlying the relationship between B-Raf-dependent ERK activation and IL-2 production, we first investigated the TCR-mediated c-Fos induction, one of the downstream targets of ERK (43). As shown in Fig. 6*A*, the expression of c-Fos was induced within 1 h, and its phosphorylation judged by electrophoretic mobility shift was potentiated by TCR stimulation in cells expressing wild-type B-Raf. There was no significant difference in c-Fos induction between Jurkat clones expressing wild-type B-Raf and B-Raf AA up to 3 h (Fig. 6*A*). Next, to examine whether B-Raf contributed to AP-1 activation, we performed a luciferase assay. Consistent with c-Fos induction, the AP-1 promoter activity in response to TCR stimulation in the Jurkat clone expressing B-Raf AA (AA2) was comparable as compared with that of the control clone (WT30) (Fig. 6*B*). Thereby, TCR-mediated c-Fos induction and AP-1 activation seemed to be less dependent on B-Raf.

B-Raf Activity Is Important for TCR-mediated NFAT Activation—The IL-2 production is regulated by nuclear translocation and activation of the NFAT transcription factor cooperating with the AP-1 components c-Fos and c-Jun (7–9). Thus, NFAT-dependent transcriptional events in T cells require the simultaneous activation of multiple Ras effectors such as the ERK and c-Jun N-terminal kinase pathways (44). We analyzed whether TCR-mediated B-Raf activity would influence NFAT activation, using an NFAT-GFP reporter. GFP expression, which is regulated by a promoter corresponding to the NFAT binding site, is increased in a TCR stimulation-dependent manner in mock-transfected cells (Fig. 7*A*, *a*). Comparable transfection efficiency was monitored by co-transfection of a DsRed expression vector (data not shown). In contrast, GFP expression was significantly suppressed in B-Raf AA-expressing cells, suggesting that B-Raf activity is important for the regulation of TCR-mediated NFAT activity. Given that B-Raf regulated TCR-mediated MEK/ERK activation in late phase, there is a possibility that B-Raf activation couples NFAT activation to MEK/ERK activation. For confirmation, we analyzed whether the inhibition of ERK activity in the late phase blocks NFAT reporter activity. As expected, the TCR stimulation-induced GFP expression was reduced by pretreatment with U0126 (Fig. 7*A*, *b*). Furthermore, similar to IL-2 production, the inhibition of NFAT reporter activity was also observed in the presence of U0126 after 2 h of TCR stimulation, although this suppression was less effective than that observed in simultaneous U0126 treatment at the beginning of the TCR stimulation. These results suggested that not only transient but also sustained ERK activation was necessary for the TCR-mediated NFAT activation.

Upon TCR stimulation, NFAT proteins are dephosphorylated by calcineurin, translocate into the nucleus, and then bind to cognate DNA elements (9). Finally, to dissect the mechanism responsible for the B-Raf mediated induction of NFAT activity, we evaluated the nuclear translocation of NFAT protein induced by TCR stimulation. As shown in Fig. 7*B*, the stimulation of mock-transfected Jurkat cells with TCR ligation drove the translocation of NFAT1 and NFAT2 into nucleus at 3 and 5 h of TCR stimulation. In contrast, the substantial nuclear translocation of NFAT1 and NFAT2 could not be observed in B-Raf AA-expressing Jurkat cells under either nonstimulated or TCR-stimulated conditions. Equal loading of nuclear protein in both cells was estimated by blotting of Lamin B as a nuclear

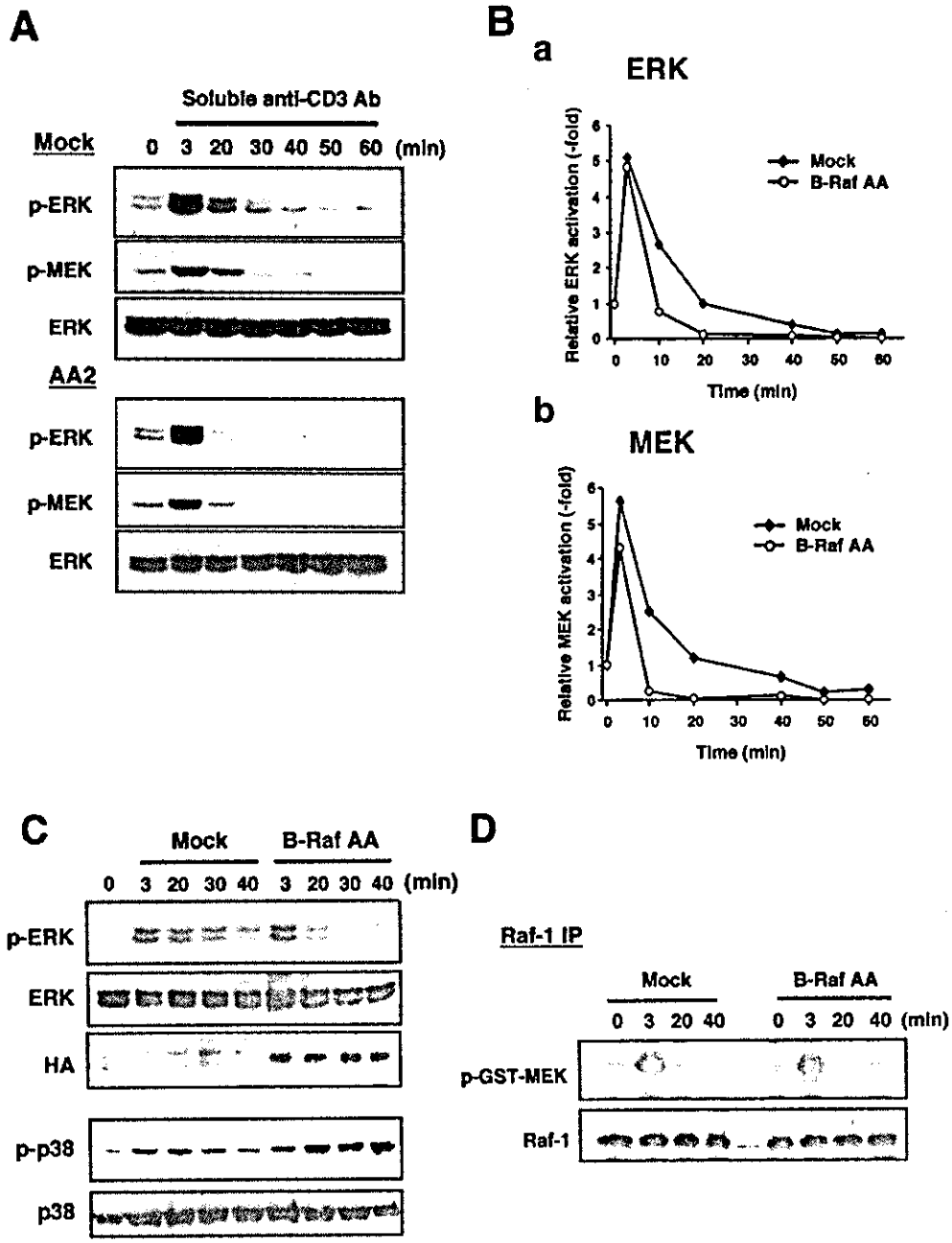

FIG. 4. **Dominant negative B-Raf AA prevented T cells from inducing sustained MEK/ERK activation in response to TCR ligation.** *A*, phosphorylation kinetics of MEK and ERK in Jurkat clones expressing wild-type B-Raf or B-Raf AA (AA2) induced by TCR cross-linking with soluble anti-CD3 antibody. *B*, kinetics of relative amount of phosphorylated ERK (*a*) and MEK (*b*). The relative value of intensity of phosphoprotein bands divided by that of whole ERK bands at each time point observed in mock- or B-Raf AA (AA2)-expressing clone were plotted. The ratio at 0 min was assigned to be 1.0. *C*, Western blotting analyses were done as described in *A* using whole cell lysates from TAg-Jurkat cells transiently transfected with mock or B-Raf AA expression vector and stimulated for the indicated times. Blottings with anti-phospho-ERK, ERK, HA (B-Raf), phospho-p38, or p38 antibodies are shown. *D*, TAg-Jurkat cells transiently transfected with mock vector or with B-Raf AA expression vector were stimulated with TCR cross-linking for the indicated times. *In vitro* kinase assays for Raf-1 were performed using immunoprecipitates from each cell extract with an anti-Raf-1 antibody (*upper panel*). Blotting with anti-Raf-1 antibody indicated equal protein loading (*lower panel*). Each result from three independent experiments was essentially the same, and one is shown.

marker. It is most likely that the defect of NFAT activity in B-Raf AA expressing cells was due to the aberrant nuclear translocation of NFAT1 and NFAT2. Accordingly, these results suggest that TCR-mediated NFAT activation relies on prolonged B-Raf/MEK/ERK activation and that the attenuation of NFAT activation by B-Raf AA reflects the inhibition of TCR-stimulated IL-2 production.

DISCUSSION

Although it is well known that receptor-mediated signals activate the Raf/MEK/ERK cascade, the precise mechanisms of how the TCR signal provokes the cellular response through Raf/MEK/ERK activation remain to be investigated. In mouse models, both Raf-1- and B-Raf-deficient mice resulted in embryonic lethality (20, 45), indicating conclusively that the functions of both Raf isoforms for embryogenesis are not completely overlapping. However, it is poorly understood whether the three Raf isoforms have functional redundancy or if the Raf isoforms play a specific role(s) in T cell activation. Until recently, Raf-1 has been considered to be a major signaling mediator for MEK/ERK activation in TCR-stimulated T cells (27, 46). Our observations provided evidence that the functions of

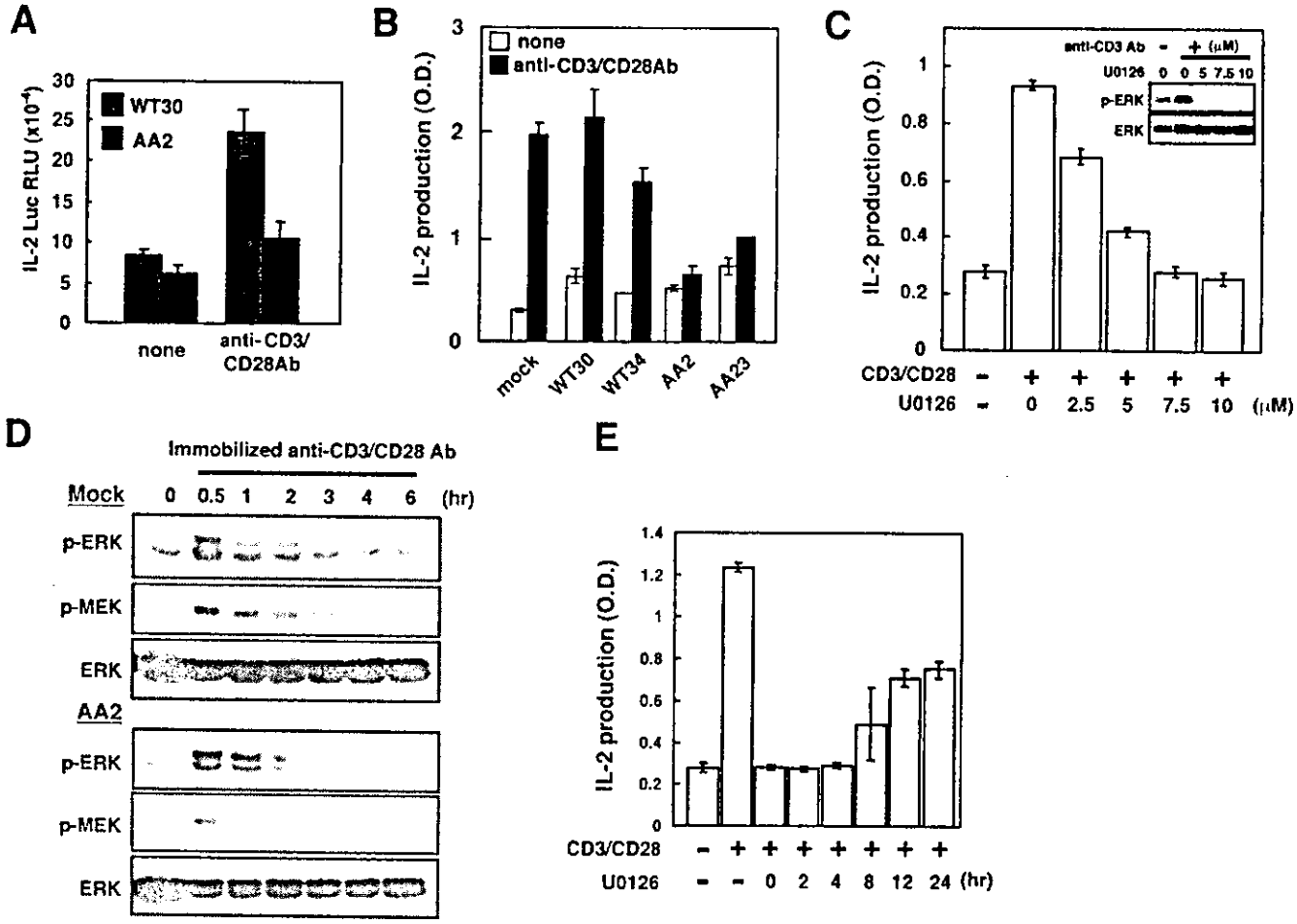

FIG. 5. **Sustained ERK activation controlled by B-Raf is critical in TCR-mediated production of IL-2.** *A*, luciferase assay for IL-2 promoter activity. Jurkat clone expressing wild-type B-Raf (WT30) or B-Raf AA (AA2) was transfected with an IL-2-luciferase construct and incubated with or without immobilized anti-CD3 and anti-CD28 antibodies for 12 h. Each luciferase activity was evaluated and normalized by the co-transfected β-galactosidase activity. *RLU*, relative luciferase unit. *B*, Jurkat clones expressing wild-type B-Raf (WT30 and WT34), B-Raf AA (AA2 and AA23), and mock-transfectant were stimulated with immobilized anti-CD3 and anti-CD28 antibodies for 48 h. IL-2 in the culture supernatants was measured by enzyme-linked immunosorbent assay. *C*, Jurkat cells were pretreated with MEK inhibitor U0126 at the indicated concentrations for 30 min before stimulation and then were stimulated with an anti-CD3 antibody for 3 min, and phosphorylation of ERK was analyzed with Western blotting (*insets*). For measurement of IL-2, Jurkat cells pretreated with U0126 at the indicated concentrations were stimulated with immobilized anti-CD3 and anti-CD28 antibodies for 48 h. IL-2 in the culture supernatants were measured by enzyme-linked immunosorbent assay. *D*, mock-transfected (*upper panel*) or B-Raf AA expressing Jurkat clone (AA2; *lower panel*) were stimulated with the immobilized anti-CD3 and anti-CD28 antibodies for the indicated times. The whole cell extract from each sample was analyzed by blotting with anti-phospho-ERK (*top panel*), phospho-MEK (*middle panel*), or ERK (*bottom panel*) antibodies, respectively. *E*, vehicle (Me_2SO) or U0126 (5 μM) was added to the culture at the indicated times after the beginning of stimulation of Jurkat cells with immobilized anti-CD3 and anti-CD28 antibodies. After 48 h from the start of stimulation, each culture supernatant was harvested, and the IL-2 concentration was measured, as described in *C*. Typical data from three independent and reproducible experiments are presented here.

B-Raf for TCR-mediated activation do not entirely overlap with those of other Raf proteins. We elucidated that B-Raf activation couples Ras with TCR-mediated MEK/ERK activation and is indispensable for prolongation of substantial MEK/ERK activation *in vivo*.

This sustained MEK/ERK activation correlates with duration and strength of B-Raf activity. We considered that activation thresholds and the mechanisms regulating each Raf activity lead to distinct activation kinetics of these two Raf kinases. In agreement with this interpretation, the following observations were reported. Although the activities of both Raf-1 (47) and B-Raf (Fig. 3) were dependent on Ras activity, in addition to Ras, Src family kinases regulated Raf-1 activity (48). Upon activation, Raf-1 was shown to be phosphorylated on some tyrosine, serine, and threonine residues, which fulfill the regulatory functions, and the phosphorylation status of these sites in Raf-1 is different from that of B-Raf. First, the major target site of Src is Tyr^{340} in Raf-1; however, B-Raf activity seemed to be less dependent on Src, and Ras activation is sufficient for B-Raf function because B-Raf lacks the Tyr corresponding to Tyr^{340} in Raf-1 (41, 49). Thus, B-Raf activation requires Ras but not Src to activate MEK/ERK, whereas Raf-1 activation needs the synergy of Ras and Src tyrosine kinase(s) (41, 49). Second, conserved B-Raf Ser^{445}, corresponding to Ser^{338} in Raf-1, which is one of the regulatory phosphorylation sites of Raf activity, is constitutively phosphorylated in fibroblasts (49). These results seem to explain the fact that B-Raf exhibits a higher intrinsic kinase activity in a quiescent situation and, once stimulated, a longer activation period than does Raf-1 in our system and other systems.

It should be noted that the dominant negative mutant of B-Raf (B-Raf AA) did not impair the transient MEK/ERK activation but did suppress the sustained MEK/ERK activation although B-Raf was activated and associated with MEK in both the early and the late phase after TCR stimulation. Why was not MEK/ERK activation in the early phase drastically attenuated by B-Raf AA? The most likely explanation is that Raf-1 can compensate for the defects of B-Raf activation due to the

functional redundancy between Raf-1 and B-Raf in early phase. The idea was supported by our observations; the B-Raf AA did not grossly perturb ERK activation when Raf-1 was active in 3–20 min after TCR stimulation (Figs. 2 and 4), suggesting that Raf-1 activity is sufficient to induce ERK activation in the early phase. On the other hand, ERK activation in the late phase (~20 min) was abrogated by B-Raf AA, because the kinase activity of Raf-1 declined, and Raf-1 could no longer compensate for B-Raf activity. Consequently, although we could not exclude the possibility that Raf-1 activity in early phase modulates the TCR-mediated B-Raf activation, our observations led to the model that Raf-1 activity is responsible and sufficient for the early phase MEK/ERK activation, whereas B-Raf activity is essential for the late phase MEK/ERK activation in TCR-stimulated T cells.

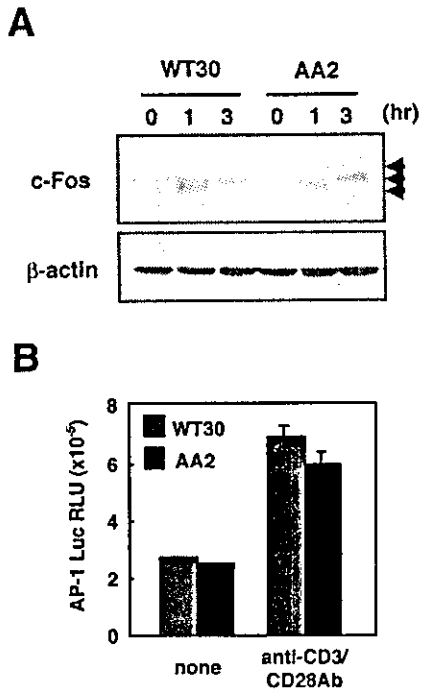

FIG. 6. **B-Raf activity does not influence c-Fos induction and AP-1 activation.** *A*, Western blotting analysis using an anti-c-Fos antibody (*upper panel*). Jurkat clones expressing wild-type B-Raf (WT30) or B-Raf AA (AA2) were stimulated with immobilized anti-CD3 antibody for the indicated times. Blotting with an anti-β-actin antibody indicated equal loading of proteins (*lower panel*). The *arrowheads* indicate the phosphorylated forms of c-Fos. *B*, luciferase assay for AP-1 promoter activity. Jurkat clones expressing wild-type B-Raf (WT30) or B-Raf AA (AA2) together with an AP-1-luciferase construct were stimulated with immobilized anti-CD3 and anti-CD28 antibodies for 8 h followed by a 12-h culture. Each luciferase activity was measured and normalized by the co-transfected β-galactosidase activity. *RLU*, relative luciferase unit. The data are representative of three independent and reproducible experiments. *Ab*, antibody.

ERK activation is critical for the precise outcome of T cell activation, including IL-2 production (7, 15). The marked decrease in IL-2 production in T cells by the expression of B-Raf AA and by the inhibition of the late phase ERK activation using U0126 leads to the conclusion that ERK activation in the late phase regulated by B-Raf was critical for the full IL-2 production in response to TCR stimulation. In view of no defect of TCR-mediated c-Fos induction and AP-1 activation in Jurkat cells expressing B-Raf AA, it was indicated that these events were less dependent on B-Raf activity. In contrast to AP-1 activation, we found that B-Raf AA inhibited TCR-mediated nuclear translocation of NFAT and NFAT-mediated reporter activation (Figs. 6 and 7). The correlation between B-Raf and these transcriptional factors was also noted by Brummer *et al.* (24), who reported that in B-Raf null chicken B cells, B cell receptor-mediated ERK activation was eliminated in only late phase, whereas c-Fos induction was not abrogated. On the contrary, the loss of B-Raf expression resulted in significant defects in the B cell receptor-mediated activation of NFAT transcription factor, suggesting that NFAT activation is regulated by B-Raf in chicken B cells. The selective role of TCR-mediated B-Raf activation in NFAT regulation was consistent with that observed in B cells, and their regulatory mechanisms may be conserved between immunoreceptor-mediated activation in both B and T cells. These results suggest that NFAT-responsible transcriptions and subsequent IL-2 production were dependent on B-Raf and that Raf-1-induced ERK activation in the early phase is not sufficient to provoke these immunoreceptor-mediated activations.

It was expected that the inhibitory effect of B-Raf AA on NFAT activation was due to a defect in sustained ERK activation mediated by B-Raf, because the treatment of Jurkat cells with MEK inhibitor also reduced the NFAT activation. Evi-

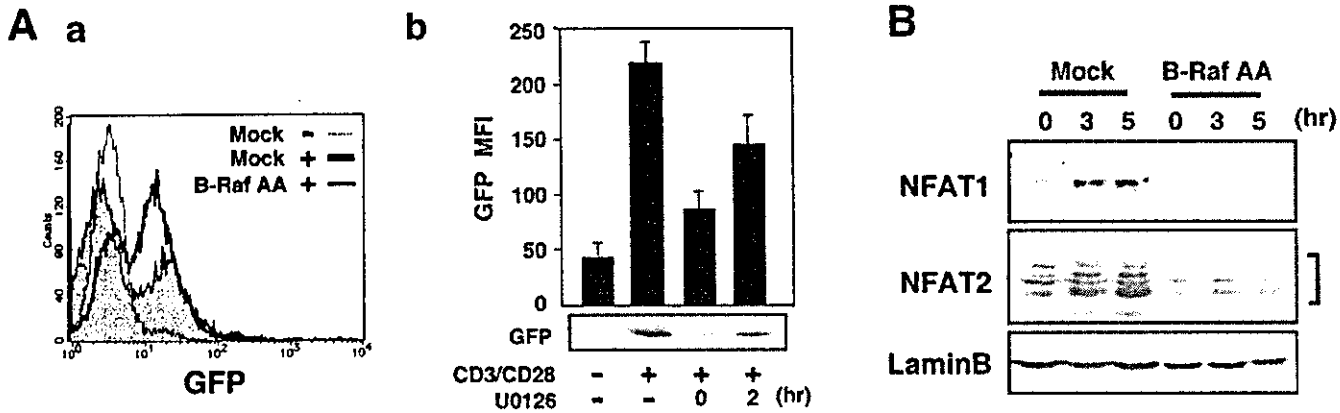

FIG. 7. **B-Raf activity is required for NFAT activation.** *A*, *a*, TAg-Jurkat cells co-transfected with the NFAT-GFP reporter construct and mock or B-Raf AA expression vector were stimulated with (+) or without (−) immobilized anti-CD3 and anti-CD28 antibodies for 9 h. A representative flow cytometric profile for GFP expression is shown. *b*, NFAT-GFP-transfected Jurkat cells were stimulated, and then GFP expression was examined by blotting with anti-GFP antibody (*lower panel*) and flow cytometry (*upper panel*). The *diagram* represents the average of GFP mean fluorescence intensity (*MFI*) obtained from three independent experiments. U0126 (5 μM) was added to the culture at 0 or 2 h after TCR stimulation. *B*, nuclear extracts were isolated from mock- or B-Raf AA-transfected cells stimulated with or without immobilized anti-CD3 and anti-CD28 antibodies for indicated times. Then, the nuclear fractions were separated by SDS-PAGE, and the translocations into nucleus of NFAT1 and NFAT2 were analyzed by Western blotting. Blotting with anti-Lamin B antibody indicated the appropriate nuclear fractionation and protein loading. Essentially similar results were obtained in three independent experiments.

dence has been accumulated that supports the contribution of ERK signaling to NFAT activation. In T cells, the transcriptional activity of NFAT was reported to be regulated by Ras/MEK/ERK acting in synergy with a calcium/calmodulin phosphatase, calcineurin (7, 44). Moreover, the mechanism by which some kinases and phosphatases regulate the NFAT activity implies modulation of nuclear translocation of this factor, its binding to DNA, or transactivation of its target gene expression. Because B-Raf AA abrogated the nuclear localization and transcriptional activity of NFAT, we propose that the model that sustained B-Raf/MEK/ERK activation modulating NFAT-dependent transcription could be achieved by regulation of intrinsic nuclear translocation of NFAT. Supporting this interpretation, it has been reported that ERK1 overexpression augmented the DNA binding activity of NFAT, resulting in NFAT activation in Jurkat cells (50). However, it has been shown that activated ERK binds to and phosphorylates NFAT2, which negatively regulates nuclear translocation and activation of NFAT2 in fibroblasts (51). Conversely, in Jurkat cells, we observed the attenuation of TCR-stimulated nuclear translocation of NFAT by MEK inhibitor.[2] These seemingly discrepant results might be accounted for by use of different systems and cell types. In any case, the formal demonstration of a role for B-Raf and ERK in the regulation of NFAT activation *in vivo* requires more detailed analysis.

It is noteworthy that temporal difference in the Raf-induced ERK activation signal induces qualitatively different cellular responses. In PC12 cells, epidermal growth factor-driven proliferation was coupled with transient ERK activation. On the contrary, neural growth factor-driven differentiation of PC12 cells into sympathetic neurons was induced by sustained ERK activation (10), which was mediated by B-Raf (23). A similar phenomenon was found in T cells. Mariathasan *et al.* (52) demonstrated that in thymocytes, negatively selecting stimuli by agonistic peptides through TCR induced transient and strong ERK activation, resulting in cell death, whereas positively selecting stimuli by the analogue peptides induced sustained and weak ERK activation, resulting in cell survival. In a very recent study, it has been reported that B-Raf but not Raf-1 was activated with TCR stimulation in $CD4^+CD8^+$ double positive thymocytes (53). These observations and our findings that B-Raf and Raf-1 activities regulated the strength and the duration of TCR-mediated ERK activation prompted us to consider that the Ras/B-Raf/MEK/ERK pathway also could play important roles in determining the cell fate such as thymocyte differentiation regulated by temporally distinct ERK activity.

In summary, our data suggest that Ras/B-Raf/MEK/ERK can serve as a novel component of signaling pathways that regulate the duration of ERK activity in response to TCR stimulation. B-Raf and ERK activation with a proper duration determines biological outcomes such as IL-2 production in human T cells.

Acknowledgments—We thank Dr. K. L. Guan for generously providing B-Raf constructs, Dr. V. A. Boussiotis for the IL-2 promoter-luciferase reporter construct, Dr. R. M. Niles for the AP-1-luciferase reporter construct, Dr. T. Saito for the NFAT-GFP reporter construct, Dr. Y. Takai for the GST-MEK expression construct, and Dr. G. R. Crabtree for the TAg-Jurkat cells. We also thank M. Ohara for helpful comments.

REFERENCES

1. Kane, L. P., Lin, J., and Weiss, A. (2000) *Curr. Opin. Immunol.* **12,** 242–249
2. Genot, E., and Cantrell, D. A. (2000) *Curr. Opin. Immunol.* **12,** 289–294
3. D'Ambrosio, D., Cantrell, D. A., Frati, L., Santoni, A., and Testi, R. (1994) *Eur. J. Immunol.* **24,** 616–620
4. Carey, K. D., Dillon, T. J., Schmitt, J. M., Baird, A. M., Holdorf, A. D., Straus, D. B., Shaw, A. S., and Stork, P. J. (2000) *Mol. Cell. Biol.* **20,** 8409–8419
5. Katagiri, K., Hattori, M., Minato, N., and Kinashi, T. (2002) *Mol. Cell. Biol.* **22,** 1001–1015
6. Rincon, M. (2001) *Curr. Opin. Immunol.* **13,** 339–345
7. Whitehurst, C. E., and Geppert, T. D. (1996) *J. Immunol.* **156,** 1020–1029
8. Faris, M., Kokot, N., Lee, L., and Nel, A. E. (1996) *J. Biol. Chem.* **271,** 27366–27373
9. Hogan, P. G., Chen, L., Nardone, J., and Rao, A. (2003) *Genes Dev.* **17,** 2205–2232
10. Marshall, C. J. (1995) *Cell* **80,** 179–185
11. Bommhardt, U., Scheuring, Y., Bickel, C., Zamoyska, R., and Hunig, T. (2000) *J. Immunol.* **164,** 2326–2337
12. van den Brink, M. R., Kapeller, R., Pratt, J. C., Chang, J. H., and Burakoff, S. J. (1999) *J. Biol. Chem.* **274,** 11178–11185
13. Pages, G., Guerin, S., Grall, D., Bonino, F., Smith, A., Anjuere, F., Auberger, P., and Pouyssegur, J. (1999) *Science* **286,** 1374–1377
14. Mariathasan, S., Ho, S. S., Zakarian, A., and Ohashi, P. S. (2000) *Eur. J. Immunol.* **30,** 1060–1068
15. Li, Y. Q., Hii, C. S., Der, C. J., and Ferrante, A. (1999) *Immunology* **96,** 524–528
16. Hagemann, C., and Rapp, U. R. (1999) *Exp. Cell Res.* **253,** 34–46
17. Magnuson, N. S., Beck, T., Vahidi, H., Hahn, H., Smola, U., and Rapp, U. R. (1994) *Semin. Cancer Biol.* **5,** 247–253
18. Eychene, A., Dusanter-Fourt, I., Barnier, J. V., Papin, C., Charon, M., Gisselbrecht, S., and Calothy, G. (1995) *Oncogene* **10,** 1159–1165
19. Barnier, J. V., Papin, C., Eychene, A., Lecoq, O., and Calothy, G. (1995) *J. Biol. Chem.* **270,** 23381–23389
20. Wojnowski, L., Zimmer, A. M., Beck, T. W., Hahn, H., Bernal, R., Rapp, U. R., and Zimmer, A. (1997) *Nat. Genet.* **16,** 293–297
21. Papin, C., Denouel-Galy, A., Laugier, D., Calothy, G., and Eychene, A. (1998) *J. Biol. Chem.* **273,** 24939–24947
22. Vaillancourt, R. R., Gardner, A. M., and Johnson, G. L. (1994) *Mol. Cell. Biol.* **14,** 6522–6530
23. York, R. D., Yao, H., Dillon, T., Ellig, C. L., Eckert, S. P., McCleskey, E. W., and Stork, P. J. (1998) *Nature* **392,** 622–626
24. Brummer, T., Shaw, P. E., Reth, M., and Misawa, Y. (2002) *EMBO J.* **21,** 5611–5622
25. Erhardt, P., Schremser, E. J., and Cooper, G. M. (1999) *Mol. Cell. Biol.* **19,** 5308–5315
26. Peraldi, P., Frodin, M., Barnier, J. V., Calleja, V., Scimeca, J. C., Filloux, C., Calothy, G., and Van Obberghen, E. (1995) *FEBS Lett.* **357,** 290–296
27. Owaki, H., Varma, R., Gillis, B., Bruder, J. T., Rapp, U. R., Davis, L. S., and Geppert, T. D. (1993) *EMBO J.* **12,** 4367–4373
28. Northrop, J. P., Ullman, K. S., and Crabtree, G. R. (1993) *J. Biol. Chem.* **268,** 2917–2923
29. Chen, Y. Z., Matsushita, S., and Nishimura, Y. (1996) *J. Immunol.* **157,** 3783–3790
30. Irie, A., Chen, Y. Z., Tsukamoto, H., Jotsuka, T., Masuda, M., and Nishimura, Y. (2003) *Eur. J. Immunol.* **33,** 1497–1507
31. van den Hoff, M. J., Moorman, A. F., and Lamers, W. H. (1992) *Nucleic Acids Res.* **20,** 2902
32. Ohtsuka, T., Shimizu, K., Yamamori, B., Kuroda, S., and Takai, Y. (1996) *J. Biol. Chem.* **271,** 1258–1261
33. Zhang, B. H., and Guan, K. L. (2000) *EMBO J.* **19,** 5429–5439
34. Boussiotis, V. A., Freeman, G. J., Berezovskaya, A., Barber, D. L., and Nadler, L. M. (1997) *Science* **278,** 124–128
35. Huang, Y., Boskovic, G., and Niles, R. M. (2003) *J. Cell. Physiol.* **194,** 162–170
36. Ohtsuka, M., Arase, H., Takeuchi, A., Yamasaki, S., Shiina, R., Suenaga, T., Sakurai, D., Yokosuka, T., Arase, N., Iwashima, M., Kitamura, T., Moriya, H., and Saito, T. (2004) *Proc. Natl. Acad. Sci. U. S. A.* **101,** 8126–8131
37. Uemura, Y., Senju, S., Maenaka, K., Iwai, L. K., Fujii, S., Tabata, H., Tsukamoto, H., Hirata, S., Chen, Y. Z., and Nishimura, Y. (2003) *J. Immunol.* **170,** 947–960
38. Vossler, M. R., Yao, H., York, R. D., Pan, M. G., Rim, C. S., and Stork, P. J. (1997) *Cell* **89,** 73–82
39. Xiang, X., Zang, M., Waelde, C. A., Wen, R., and Luo, Z. (2002) *J. Biol. Chem.* **277,** 44996–45003
40. Chong, H., Lee, J., and Guan, K. L. (2001) *EMBO J.* **20,** 3716–3727
41. Marais, R., Light, Y., Paterson, H. F., Mason, C. S., and Marshall, C. J. (1997) *J. Biol. Chem.* **272,** 4378–4383
42. Borovsky, Z., Mishan-Eisenberg, G., Yaniv, E., and Rachmilewitz, J. (2002) *J. Biol. Chem.* **277,** 21529–21536
43. Deng, T., and Karin, M. (1994) *Nature* **371,** 171–175
44. Genot, E., Cleverley, S., Henning, S., and Cantrell, D. (1996) *EMBO J.* **15,** 3923–3933
45. Wojnowski, L., Stancato, L. F., Zimmer, A. M., Hahn, H., Beck, T. W., Larner, A. C., Rapp, U. R., and Zimmer, A. (1998) *Mech. Dev.* **76,** 141–149
46. Taylor-Fishwick, D. A., and Siegel, J. N. (1995) *Eur. J. Immunol.* **25,** 3215–3221
47. Wotton, D., Ways, D. K., Parker, P. J., and Owen, M. J. (1993) *J. Biol. Chem.* **268,** 17975–17982
48. Pathan, N. I., Ashendel, C. L., Geahlen, R. L., and Harrison, M. L. (1996) *J. Biol. Chem.* **271,** 30315–30317
49. Mason, C. S., Springer, C. J., Cooper, R. G., Superti-Furga, G., Marshall, C. J., and Marais, R. (1999) *EMBO J.* **18,** 2137–2148
50. Park, J. H., and Levitt, L. (1993) *Blood* **82,** 2470–2477
51. Porter, C. M., Havens, M. A., and Clipstone, N. A. (2000) *J. Biol. Chem.* **275,** 3543–3551
52. Mariathasan, S., Zakarian, A., Bouchard, D., Michie, A. M., Zuniga-Pflucker, J. C., and Ohashi, P. S. (2001) *J. Immunol.* **167,** 4966–4973
53. Reynolds, L. F., de Bettignies, C., Norton, T., Beeser, A., Chernoff, J., and Tybulewicz, V. L. (2004) *J. Biol. Chem.* **279,** 18239–18246

[2] H. Tsukamoto, A. Irie, and Y. Nishimura, unpublished data.

Available online at www.sciencedirect.com
SCIENCE DIRECT®
Biochemical and Biophysical Research Communications 321 (2004) 432–440
BBRC
www.elsevier.com/locate/ybbrc

Detection of the novel autoantibody (anti-UACA antibody) in patients with Graves' disease

Tsuyoshi Ohkura [a], Shin-ichi Taniguchi [a,*], Kazuhiro Yamada [b], Naoko Nishio [a], Tomohisa Okamura [a], Akio Yoshida [a], Keiichi Kamijou [c], Shuji Fukata [d], Kanji Kuma [d], Yoichi Inoue [e], Ichiro Hisatome [f], Satoru Senju [g], Yasuharu Nishimura [g], Chiaki Shigemasa [a]

[a] *Division of Molecular Medicine and Therapeutics, Department of Multidisciplinary Internal Medicine, Tottori University Faculty of Medicine, Yonago 683-8504, Japan*
[b] *Department of Ophthalmology and Visual Science, Kumamoto University Graduate School of Medical Sciences, Kumamoto 860-0811, Japan*
[c] *Kamijou Thyroid Research Institute, Sapporo 060-0042, Japan*
[d] *Kuma Hospital, Kobe 650-0011, Japan*
[e] *Olympia Eye Hospital, Tokyo 150-0001, Japan*
[f] *School of Life Science, Faculty of Medicine, Tottori University, Yonago 683-8504, Japan*
[g] *Division of Immunogenetics, Department of Neuroscience and Immunology, Kumamoto University Graduate School of Medical Science, Kumamoto 860-0811, Japan*

Received 9 June 2004

Abstract

Uveal autoantigen with coiled coil domains and ankyrin repeats (UACA) is an autoantigen in patients with panuveitis such as Vogt–Koyanagi–Harada disease. The prevalence of IgG anti-UACA antibodies in patients with uveitis is significantly higher than healthy controls, suggesting its potential role as an autoantigen. Originally, UACA was cloned from dog thyroid tissue following TSH stimulation. So, we presumed UACA could be a novel autoantigen in autoimmune thyroid diseases. We measured serum anti-UACA antibody titer using ELISA in patients with autoimmune thyroid diseases (Graves' disease, Hashimoto's thyroiditis, subacute thyroiditis, and silent thyroiditis). The prevalence of anti-UACA antibodies in Graves' disease group was significantly higher than that in healthy group (15% vs. 0%). Moreover, the prevalence of anti-UACA antibodies in Graves' ophthalmopathy was significantly higher than that in Graves' patients without ophthalmopathy (29% vs. 11%). Especially, 75% of severe ocular myopathy cases showed high UACA titer. Immunohistochemical analysis revealed that UACA protein is expressed in eye muscles as well as human thyroid follicular cells. Taken together, UACA is a novel candidate for eye muscle autoantigens in thyroid-associated ophthalmopathy.

Keywords: Uveal autoantigen with coiled coil domains and ankyrin repeats; Graves' disease; Graves' ophthalmopathy; Autoantigen; Ocular myopathy; FRTL5; Vogt–Koyanagi–Harada disease; Thyroid–eye shared autoantigen

Uveal autoantigen with coiled coil domains and ankyrin repeats (UACA) is an autoantigen associated with panuveitis. Anti-UACA antibody appears in patients sera of Vogt–Koyanagi–Harada disease (VKH), sarcoidosis, and Behçet disease with uveitis. Although UACA is expressed in various tissues such as skeletal muscle and melanocyte, the appearance of anti-UACA antibody seems to reflect the autoimmune reaction against uveal melanocyte [1]. Interestingly, UACA was originally

* Corresponding author. Fax: +81-859-34-8099.
E-mail address: stani@grape.med.tottori-u.ac.jp (S. Taniguchi).

0006-291X/$ - see front matter © 2004 Elsevier Inc. All rights reserved.
doi:10.1016/j.bbrc.2004.06.162

identified from dog thyroid as one of TSH regulated genes with unknown function [2]. The dual expression of UACA in thyroid and skeletal muscle led us to the idea that UACA could be an autoantigen associated with Graves' disease, since patients with Graves' disease frequently suffer from ophthalmopathy with ocular myopathy [3–15].

Thyroid-associated ophthalmopathy (TAO) is considered to be an autoimmune disorder of eye muscle and surrounding orbital connective tissue and fat, and the current dogma tells that TAO is induced by autoimmune reaction against thyroid and orbital tissue shared antigens [3–21]. One such candidate is TSH receptor, which is expressed in the orbital preadipocyte and fibroblast [8–11]. Several eye muscle and thyroid shared antigens also have clinical relevance in TAO; flavoprotein [16,17], 1D [18], and G2s protein [22–24]. The primary reaction in ocular tissue is thought to be T-cell-mediated autoimmunity against TSH receptor (TSHR) expressed in ocular fibroblasts. The appearance of antibodies against Fp, G2s, and 1D seems to be the secondary event in TAO process, reflecting the release of sequestered cytoskeletal proteins from damaged eye muscles [23,24]. These eye muscle proteins are expressed in eye muscles as well as skeletal muscles. Since UACA is expressed in skeletal muscle as well as thyroid tissue, we presumed that the appearance of anti-UACA autoantibody could be linked to the autoimmune response associated with Graves' ophthalmopathy.

In this study, we measured serum UACA antibody titer in patients with autoimmune thyroid diseases; healthy controls, Graves' disease, Hashimoto's disease, silent thyroiditis, and subacute thyroiditis. The mean value of UACA antibody titer in the Graves' disease group was significantly higher than healthy controls, but other group was not. Moreover, high UACA titer was observed in Graves' ophthalmopathy patients with severe ocular myopathy.

This is the first report describing the presence of anti-UACA autoantibodies in patients with Graves' disease. Especially, high UACA titer appears to be associated with eye muscle damage of Graves' ophthalmopathy.

Materials and methods

Study patients. We studied 159 Graves' disease, 26 Hashimoto's thyroiditis, 20 silent thyroiditis, 11 subacute thyroiditis, and 43 controls. We explained the purpose of this study to all subjects and obtained their informed consent. Graves' disease patients consisted of untreated 122 females and 37 males. Diagnosis of Graves' disease was confirmed by elevated free T_3 level (13.61 ± 6.67 ng/dl), undetectable TSH level, and positive TSH binding inhibitory immunoglobulin and/or thyroid stimulating antibody. They had hyperthyroidism symptoms such as palpitation and body weight loss. Silent thyroiditis group consisted of 18 females and 2 males with a mean age of 38 year. Diagnosis of silent thyroiditis was confirmed by elevation of free T_3 levels (7.51 ± 2.39 ng/dl), suppressed ^{123}I uptake, and elevated thyroglobulin level. Subacute thyroiditis patients had neck pain and tenderness. They had elevated free T_3 level (8.15 ± 5.48 ng/dl), CRP and ESR level, and suppressed TSH level. Hashimoto's thyroiditis group had elevated TSH levels (69.1 ± 38.2 μU/ml) and positive thyroid TGAb (antithyroglobulin antibody). Forty three normal individuals of similar age and gender were used as controls.

Graves' group included 31 patients with ophthalmopathy (24 females and 8 males, 21–58 years old), 128 patients without ophthalmopathy. The eye changes were classified according to an activity index (AI, 0–7) proposed by a committee of the International Thyroid Associations. Patients with ophthalmopathy were defined as >AI, and patients without ophthalmopathy were defined as A0. Ophthalmologic examination, including measurement of eye muscle function and performance of orbital MRI, was carried out on patients with ophthalmopathy. The congestive changes were defined as >AI, with or without eye muscle involvement. Ocular myopathy was defined as: diplopia and reduced eye movement associated with marked increase of eye muscle volume on orbital MRI. Congestive ophthalmopathy was defined as: nil or minimal eye muscle enlargement with, usually, a fibrotic appearance, as described by Ossoinig [25], features of periorbital inflammation (e.g., chemosis, lid swelling, and conjunctival injection), and no diplopia or reduced eye movements.

Human subjects. Human thyroid tissues were obtained by the University of Tottori committee for the protection of human subjects and in accordance with the Declaration of Helsinki. Thyroid tissue sample was obtained at surgery from a Graves' disease patient. Normal thyroid tissue was obtained at autopsy from a patient without thyroid disease. Human eye muscle tissue with Graves' ophthalmopathy was obtained at surgery from a Graves' disease patient (kindly provided by Dr. Yoichi Inoue, Olympia Eye Hospital).

Preparation of glutathione-S transferase fusion protein. A 783-bp DNA fragment digested from *Homo sapiens* cDNA clone IMAGE 608930 (Embank Accession No. AA197064) corresponding to nucleotide position 3462–4245 of UACA cDNA was inserted into pGEX4T-2 vector to produce glutathione-*S* transferase (GST) UACA fusion protein. This UACA fragment covers C-terminal 261 amino acids (18.0%) of whole UACA consisting of 1449 amino acids. Plasmids with this construct were transformed in *Escherichia coli* and incubated in 500 ml Luria broth medium for 8 h at 37 °C with shaking. Then, IPTG was added at a final concentration of 0.1 mM and the preparation was incubated for 16 h at 25 °C with shaking. This suspension was centrifuged and the pellet was suspended in 20 ml lysis buffer [50 mM Tris–HCl (pH 7.5), 25% sucrose]. Then, we added 100 μl of 10% Nonidet P-40, 1 M $MgCl_2$ on ice. The lysate was sonicated, centrifuged, and then the supernatant was incubated with 2 ml of slurry of glutathione–Sepharose 4B for 2 h at 4 °C. This suspension was centrifuged and the pellet was washed in WE buffer [20 mM Tris–HCl (pH 7.5), 2 mM $MgCl_2$, and 1 mM DTT] 10 times. The fusion protein was eluted with G buffer [5 mM GSH, 50 mM Tris–HCl (pH 9.6)] and eluted protein concentration was estimated by Bio-Rad Protein Assay kit (Bio-Rad, Hercules, CA).

Enzyme-linked immunosorbent assay. Detection and titration of antibody to a fragment of UACA were examined using indirect enzyme-linked immunosorbent assay (ELISA). GST–UACA fusion protein and GST protein were prepared and used as antigens. Microtiter plates (96-well) (NUNC, Denmark) were coated with GST–UACA fusion protein in PBS (pH 7.4) for 15 h at 4 °C. GST protein was simultaneously coated in different wells as control. The plates were then washed with 5% skim milk/PBS for 2 h at room temperature. The plates were washed with PBS-T and incubated for 15 h at 4 °C with serum samples diluted at 1:50 with 1% skim milk/PBS. The plates were washed in PBS-T, and 100 μl of HRP-conjugated mouse anti-human IgG diluted at 1:2000 with 1% skim milk/PBS was added to each well followed by incubation at room temperature for 2 h. The plates were washed with PBS-T, and 100 μl solution of *o*-phenylenediamine (Sigma Fast; Sigma Chemical, St. Louis, MO) was added to each well. After

30 min, the reaction was stopped by adding 50 μl of 3 M H_2SO_4, and OD 490 nm was determined using a Model 550 microplate reader (Bio-Rad, Hercules, CA). The specific corrected OD value of an individual sample was calculated by subtracting the OD value of GST protein coated well from that of GST–UACA fusion protein.

Cell culture. FRTL-5 rat thyroid cells (Interthyr Research Foundation, Baltimore, MD; ATCC No. CRL 8305) were a fresh subclone (F1) that had all properties previously detailed. All cells were grown in 6H medium consisting of Coon's modified F12 (Sigma Chemical, St. Louis, MO) supplemented with 5% calf serum, 1 mM non-essential amino acids (Gibco, Grand Island, NY), and a mixture of six hormones:bovine TSH (1×10^{-10} M), insulin (10 μg/ml), cortisol (0.4 ng/ml), transferrin (5 μg/ml), glycyl-L-histidyl-L-lysine acetate (10 ng/ml), and somatostatin (10 ng/ml). Fresh medium was replaced every 2 or 3 days, and cells were passaged every 7–10 days. In different experiments, cells were maintained in 5H medium without TSH and then exposed to TSH for appropriate time period (0, 3, 6, 12, and 24 h). In dose course analysis, FRTL5 cells were incubated with various concentrations (0, 10^{-3}, 10^{-2}, 10^{-1}, and 1 mU/ml) of TSH for 24 h.

The following human thyroid cancer cell lines were obtained from Dr S. Kosugi (Department of Laboratory Medicine and Clinical Genetics Unit, Kyoto University School of Medicine); NPA [26] and FRO [27] thyroid cancer cell lines were grown in RPMI medium 1640 (31800-022, Gibco-BRL, USA) supplemented with 10% fetal calf serum, 100 U/ml penicillin, and 50 μg/ml streptomycin. FRO cells, derived from a poorly differentiated follicular thyroid carcinoma, were characterized by the presence of wild-type p53 alleles for exons 5–8 [24]. 8505C [28] and HTC [29] thyroid cancer cell lines were grown in Dulbecco's modified Eagle's medium (DMEM) (12800-017, Gibco-BRL, USA) supplemented with 10% fetal calf serum, 100 U/ml penicillin, and 50 μg/ml streptomycin. Culture medium was changed every 2 days and cells were passaged every 5–6 days.

Western blot analysis. Cells were lysed on ice in 0.6 ml lysate mix containing 1% NP40, 0.5% sodium deoxycholate, 0.1% SDS, 10 μg/ml aprotinin, 10 μg/ml leupeptin, 10 μg/ml pepstatin, and 1 mM phenylmethylsulfonyl fluoride in PBS. For immunoblotting, 10 μg of each sample was electrically transferred to Immunobilon PVDF (polyvinylidene difluoride) Transfer Membranes (Millipore, Bedford, MA). Membranes were incubated in blocking buffer; Tris-buffered saline (TBS; Tris–HCl 10 mM, pH 8.0, and NaCl 150 mM) containing 0.05% [vol/vol] Tween 20 and 5% [wt/vol] non-fat dried milk for overnight. Membranes were then incubated in blocking buffer with rabbit polyclonal anti-UACA antibody (kindly provided by Dr. K. Yamada) (1:500 dilution) or goat polyclonal anti-actin antibody (sc-1616, Santa Cruz Biotechnology, USA) for 45 min, and then washed twice with TBS containing 0.05% Tween 20. Membranes were incubated in blocking buffer with horseradish peroxidase-conjugated anti-rabbit IgG antibody for UACA or horseradish peroxidase-conjugated anti-goat IgG antibody (Amersham, UK) for actin, respectively, washed three times with TBS with 0.05% Tween 20, and then detected with enhanced chemiluminescence reagents (Amersham, UK).

Reverse transcription-PCR. Poly(A)$^+$ RNA were purified from 10 μg of each total RNA and subjected to cDNA synthesis, using random primers and Superscript reverse transcriptase. Gene-specific PCR primers were designed to amplify fragments of 505 bp and used in the reverse transcription-PCR (RT-PCR) (94 °C 30 s, 56 °C 30 s, and 74 °C 4 min, 30 cycles). Forward and reverse primer sequences for PCR amplification of UACA were 5′-GAGAAAAGAAGTTGGAATCAT AA-3′ and 5′-TTGTGTAGGTGAGTTGGGAAAG-3′, respectively.

Immunohistochemical evaluation of UACA expression. UACA expression was analyzed by immunocytochemical staining of Graves' thyroid tissues, eye muscle tissue obtained from a patient with Graves' ophthalmopathy. We immunostained the ocular tissue including extraocular muscles. Paraffin-embedded tissue section, 4-μm thick, was deparaffinized in xylene, rehydrated through a graded alcohol series to deionized water. The endogenous peroxidase activity was blocked with H_2O_2. The tissue section was incubated with rabbit polyclonal anti-UACA antibody (1:10) for 12 h at 4 °C, then washed and incubated with biotinylated horse anti-rabbit IgG (1:3000) for 30 min at room temperature. The sections were immersed in a solution with the avidin-biotin complex (Vector Laboratories, USA) for 30 min, developed with diaminobenzidine, and counterstained with eosin. The sections were scanned at magnification (200×, 400×) using light microscopy. Normal thyroid sample was obtained at autopsy from a patient without thyroid disease.

Immunofluorescent staining and microscopy. FRTL5 cells were plated on coverslips and cultured in Coon's modification HamF 12 with 5% fetal calf serum, then washed twice with PBS, and fixed with 2% paraformaldehyde. Cells were permeabilized with 0.5% Triton X-100, incubated with rabbit polyclonal anti-UACA antibody (1:100), and then visualized using FITC-conjugated anti-rabbit IgG antibody. In order to observe the fine localization of UACA protein within cells, we used confocal microscopy system (FLUOVIEW-OLYMPUS).

Statistical analysis. We used the χ^2 test (with Yeasts' correction for small numbers) and Fisher's exact test for categorical comparisons of the data. Differences in the means of continuous measurements were statistically analyzed using ANOVA. P value of <0.05 was considered to indicate statistical significance. All statistical analyses were performed on a personal computer with the statistical package StatView 5.0 for Macintosh (SAS Institute, Cary, NC).

Results

ELISA

We measured serum UACA antibody titer in patients with autoimmune thyroid diseases in ELISA, using recombinant C-terminal 18% fragment of human UACA protein. We measured titer of healthy controls (43 cases), Graves' disease (159 cases), Hashimoto's disease (26 cases), silent thyroiditis (20 cases), and subacute thyroiditis (11 cases). To exclude the effect of reactivity against GST protein, we used GST–UACA fusion protein and GST protein for ELISA, simultaneously. Evaluation of IgG anti-UACA autoantibodies was determined by subtracting the reactivities against GST from those against GST–UACA. The mean OD value of anti-UACA autoantibodies in Graves' patients was significantly higher than that in healthy controls (ANOVA; $P < 0.01$) (Fig. 1A). This group patient did not accompany VKH disease or other uveitis. In contrast, Hashimoto's thyroiditis, silent thyroiditis, and subacute thyroiditis group did not show any statistical significance compared with control. The cutoff OD value for positivity of anti-UACA IgG antibodies was defined as the mean value +3 SD of healthy controls (0.53). We found anti-UACA IgG antibodies in 15% (24/159) of Graves' patients and 0% (0/43) of healthy control (Table 1). The prevalence of IgG anti-UACA antibodies in Graves' patients was significantly higher than that in healthy control (Fisher's exact test; $P < 0.05$). Anti-UACA antibodies were found in 4% (1/26) of Hashimoto's thyroiditis, 5% (1/20) of silent thyroiditis, and 8% (1/11) of subacute thyroiditis group. The differences in prevalence of anti-UACA antibodies

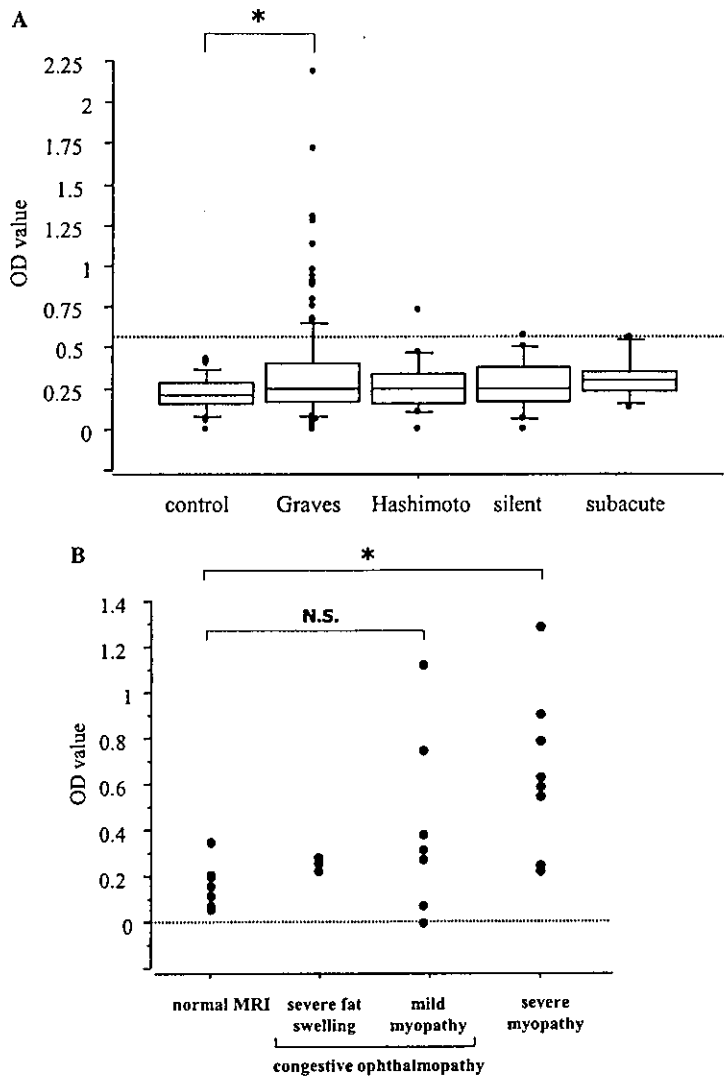

Fig. 1. (A) Distribution of anti-UACA IgG autoantibodies titer in healthy controls (control), in patients with Graves' disease (Graves), Hashimoto's disease (Hashimoto), silent thyroiditis (silent), and subacute thyroiditis (subacute). The titers of autoantibodies are expressed in the OD units. Broken line indicates a cutoff level for the positivity of autoantibody. The OD value subtracted GST protein from GST–UACA fusion protein in 159 Graves' disease samples was 0.339 ± 0.305 (mean ± SE), in 26 Hashimoto's thyroiditis samples was 0.269 ± 0.151 (mean ± SE), in 20 silent thyroiditis samples was 0.269 ± 0.156 (mean ± SE), in 11 subacute thyroiditis samples was 0.315 ± 0.130 (mean ± SE), and in 43 healthy control samples was 0.218 ± 0.103 (mean ± SE). The OD value for GST–UACA fusion protein to GST protein in 27 positive samples was 0.865 ± 0.384 (mean ± SE), and in negative samples was 0.240 ± 0.125 (mean ± SE). *Significant difference ($P < 0.01$) compared with control (ANOVA). (B) Distribution of anti-UACA IgG autoantibodies titer in patients with Graves' ophthalmopathy. The clinical manifestations of Graves' ophthalmopathy are classified into the following four groups; normal MRI, congestive ophthalmopathy with severe fat swelling, congestive ophthalmopathy with mild myopathy, and severe myopathy. The OD value subtracted GST protein from GST–UACA fusion protein in seven normal MRI samples was 0.167 ± 0.098 (mean ± SE), in three congestive ophthalmopathy with severe fat swelling samples was 0.255 ± 0.029 (mean ± SE), in seven congestive ophthalmopathy with mild myopathy samples was 0.418 ± 0.395 (mean ± SE), and in eight severe myopathy samples was 0.656 ± 0.349 (mean ± SE). *Significant difference ($P < 0.005$) compared with normal MRI (ANOVA). NS: not significant.

were not statistically significant between Hashimoto's thyroiditis and healthy control, silent thyroiditis and healthy control, and subacute thyroiditis and healthy control. More than half of Graves' patients with positive titer showed higher titer than patients with VKH disease. Positive patient sera with VKH disease showed about 0.5 OD value in the same ELISA.

Clinical manifestation

We investigated clinical manifestation of Graves' patients with high anti-UACA titer in detail. We found 37.5% (9/24) cases had ophthalmopathy. Especially, patient samples with severe eye muscle inflammation showed high anti-UACA titer. Nine cases with Graves'

Table 1
Prevalence of IgG anti-UACA autoantibodies evaluated by ELISA in sera from patients with thyroid diseases and healthy controls

Disease	Anti-human UACA IgG positive donors		P value
Graves' disease	24/159	15%	$P < 0.01$
Hashimoto's disease	1/26	4%	
Silent thyroiditis	1/20	5%	
Subacute thyroiditis	1/11	9%	
Healthy controls	0/43	0%	

Differences in prevalence of IgG anti-UACA autoantibodies are statistically significant between patients with Graves' disease and healthy controls using Fisher's exact test (2 × 2 table).

ophthalmopathy showed high titer (OD value >0.53) within 31 Graves' ophthalmopathy cases. The prevalence of anti-UACA antibodies was 29% in Graves' ophthalmopathy cases. But, the prevalence of anti-UACA antibodies in patients without ophthalmopathy was 11% (15/128). The prevalence of Graves' ophthalmopathy cases was significantly higher than that of Graves' patients without ophthalmopathy (Fisher's exact test; $P < 0.05$) (Table 2). Within nine cases of high titer, six cases showed severe eye muscle inflammation in MRI study. Graves' ophthalmopathy is classified into the following four groups; severe ocular myopathy, congestive ophthalmopathy with mild myopathy, congestive ophthalmopathy with severe orbital fat swelling and without myopathy, and normal MRI. The prevalence of anti-UACA antibodies was 75% (6/8) in severe ocular myopathy, which had severe eye muscle enlargement and high intensity signal within eye muscle in T2WI MRI study. In contrast, the prevalence of anti-UACA antibodies was 28% (2/7) in congestive ophthalmopathy cases with mild myopathy, who had mild eye muscle enlargement and high intensity signal in T2WI MRI study. The prevalence of anti-UACA antibodies was 0% (0/3) in congestive ophthalmopathy case, who had severe orbital fat swelling, no eye muscle enlargement, and no high intensity in T2WI MRI study. UACA titer of seven patients with normal MRI study was all normal.

The mean UACA titer of severe ocular myopathy cases was significantly higher than that of seven normal cases in MRI study (ANOVA; $P < 0.005$) (Fig. 1B). The prevalence of anti-UACA antibodies was 75% (6/8) in patients with severe ocular myopathy. The prevalence was significantly higher than that of normal MRI group (Fisher's exact test; $P < 0.01$) (Table 3). But, any other group did not show the significant difference compared with normal MRI group.

Table 2
Prevalence of IgG anti-UACA autoantibodies evaluated by ELISA in sera from patients with Graves' ophthalmopathy and without Graves' ophthalmopathy

Group	Anti-human UACA IgG positive donors		P value
Graves' ophthalmopathy (+)	9/31	29%	$P < 0.05$
Graves' ophthalmopathy (−)	15/128	11%	

Statistical analyses refer to differences between patients with Graves' ophthalmopathy and without Graves' ophthalmopathy determined using χ^2 test (2 × 2 table, Yeasts' correction for small numbers).

Table 3
Prevalence of IgG anti-UACA autoantibodies evaluated by ELISA in sera from patients with Graves' ophthalmopathy and MRI study

Group	Anti-human UACA IgG positive donors		P value
Severe ocular myopathy	6/8	75%	$P < 0.01$
Congestive ophthalmopathy (with mild myopathy)	2/7	28%	
Congestive ophthalmopathy (with severe orbital fat swelling)	0/3	0%	
Normal MRI	0/7	0%	

Statistical analyses refer to differences between patients with severe ocular myopathy and Normal MRI group determined using Fisher's exact test (2 × 2 table).

Expression of UACA in thyroid

To examine mRNA expression of UACA in thyroid, we performed RT-PCR analysis (Fig. 2C). Gene-specific PCR primers were designed to amplify 505 bp fragments of C-terminal portion of human UACA cDNA. The expression of UACA mRNA was observed in all human thyroid cancer cell lines (HTC, 8505C, FRO, and NPA), as well as human thyroid tissue of Graves' disease, Hashimoto's thyroiditis, and normal control. This result indicates UACA mRNA is expressed in human thyroid follicular cells.

To examine the expression profile of UACA protein in FRTL5 cell, we performed Western blot analysis. UACA encoded 160 kDa protein (Figs. 2A and B). The amount of UACA protein was augmented in a time (0, 3, 6, 12, and 24 h) (Fig. 2A) and dose-dependent manner following TSH stimulation (0, 10^{-3}, 10^{-2}, 10^{-1}, and 1 mU/ml) (Fig. 2B). In a time course, UACA protein increased after 3 h following TSH stimulation. The strongest signal was observed after 6 or 12 h following TSH stimulation, and the signal decreased after 24 h following TSH stimulation. In a dose course of TSH, the minimum concentration of TSH to increase UACA protein was 10^{-3} mU/ml.

In order to study the cytochemical localization of UACA, we estimated the expression of UACA in FRTL5 cells. The UACA protein was weakly expressed both in nucleus and cytoplasm of cells in the absence of TSH (Fig. 3A). Interestingly, TSH stimulation recruited UACA into nucleus (Fig. 3A; 24 h). In order to observe the fine localization of UACA within TSH-stimulated

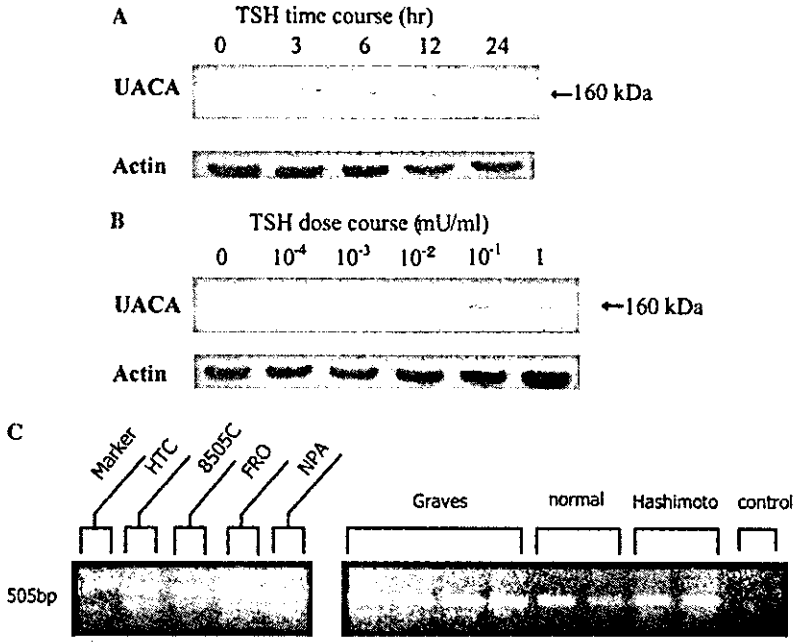

Fig. 2. TSH potentiates UACA protein expression in FRTL5 thyroid cells: (A) time sequence, (B) dose dependency. FRTL5 cells were preincubated in 5H medium with 5% CS for 5–6 days and then incubated with appropriate concentrations of TSH. To ensure the total amount of protein in each lane was identical, membranes were simultaneously incubated with anti-actin antibody (1:250 dilution). (C) RT-PCR analysis using human UACA-specific primers revealed the expression of UACA mRNA in human thyroid cancer cell lines (HTC, 8505C, FRO, and NPA), and the thyroid tissue of Grave's disease, Hashimoto's disease, and normal subject. Control lane indicates PCR product when any template was not included in PCR.

FRTL5, we used a differential interference contrast image. Most of the UACA fluorescence was localized within nucleus, whereas less was localized in cytoplasm (Fig. 3B). To examine UACA expression in human thyroid tissue, we then carried out an immunohistochemical analysis using rabbit polyclonal anti-UACA antibody. In thyroid tissue of Graves' disease, UACA appeared to be expressed in the nucleus of thyroid follicular cells (Fig. 3C).

Expression of UACA protein in eye muscle

In order to investigate the association of Graves' ophthalmopathy and anti-UACA antibody production, we examined UACA expression in human eye muscle derived from a patient with Graves' ophthalmopathy. In human eye muscle tissue with Graves' ophthalmopathy, UACA protein was exclusively expressed in eye muscle fiber (arrow), but UACA expression was relatively weak in surrounding orbital connective tissue and fat (Fig. 3D). The eye muscle sample was derived from a patient with Graves' ophthalmopathy, who was already treated by methimazole and corticosteroid. Since this pretreatment may modify the UACA expression in eye muscle, we simultaneously examined UACA expression in normal rat eye muscle. UACA protein was expressed in normal rat eye muscle fiber as observed in the human sample (data not shown). This result indicates UACA is expressed in eye muscle fiber as well as thyroid cells, which are the autoimmune target tissues in Graves' disease.

Discussion

UACA is a protein cloned by serological analysis of recombinant cDNA expression libraries (SEREX) method with serum samples obtained from patients with VKH disease, to identify the target autoantigens in VKH disease [1]. VKH disease is recognized as an autoimmune systemic disorder. In VKH, inflammatory disorders in multiple organs include melanocytes, uvea (resulting in acute bilateral panuveitis), skin (vitiligo and alopecia), central nervous system (meningitis), and inner ears (hearing loss and tinnitus). These inflammatory aspects are attributed to the immunological destruction of melanocytes. The prevalence of IgG anti-UACA autoantibodies is 19.6% in patients with VKH, and 0% in the healthy controls, 28.1% in patients with Behçet disease, and 21.1% in patients with sarcoidosis, so anti-UACA autoantibodies are considered as one of the autoantibodies in these panuveitis diseases. Originally, UACA was cloned from dog thyroid tissue following TSH stimulation, so we presumed UACA could be a novel candidate of autoantigen in autoimmune thyroid diseases [2]. Then, we analyzed the

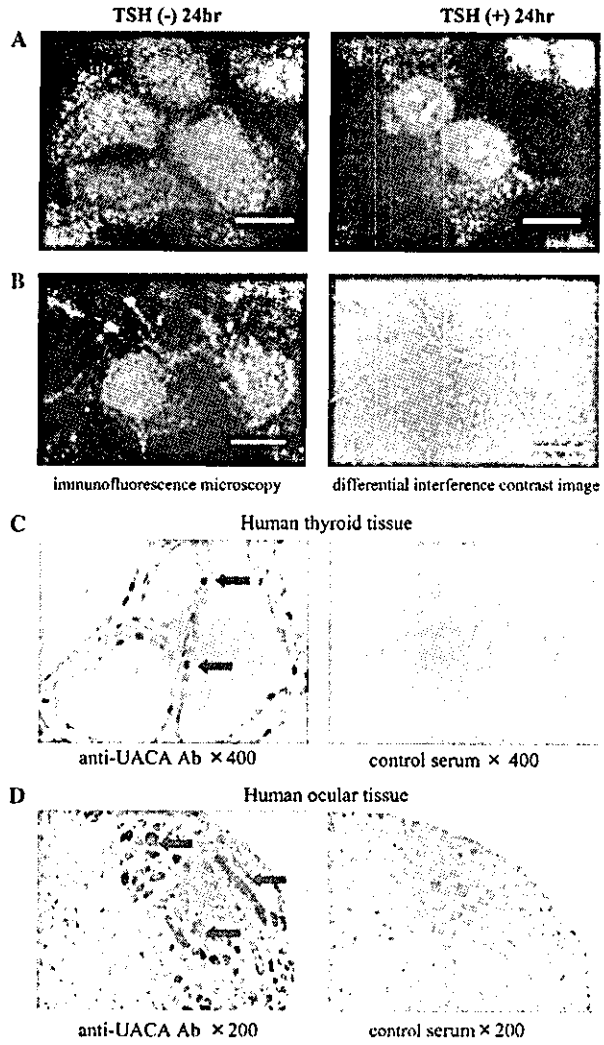

Fig. 3. (A) The cytochemical localization of UACA protein in FRTL5 cells in the absence or presence of TSH (1 mU/ml, 24 h). Inserted bar indicates 10 μm. (B) The fine cytochemical localization of UACA protein in FRTL5 cells followed by TSH stimulation (TSH 1 mU/ml, 24 h). Differential interference contrast image (right panel), and immunofluorescence microscopy image of FRTL5 cells (left panel). Inserted bar indicates10 μm. (C) The expression of UACA protein in human thyroid tissue of Graves' disease. Immunohistochemical analysis was done using rabbit anti-UACA antibodies. The sections were scanned at magnification (400×) using light microscopy. The arrows indicate nucleus of thyroid follicular cell expressing UACA protein. (D) The expression of UACA protein in human eye muscle tissue with Graves' ophthalmopathy. The sections were scanned at magnification (200×) using light microscopy. The arrows indicate eye muscle fibers expressing UACA proteins.

presence of anti-UACA antibodies in autoimmune thyroid diseases.

In ELISA study, the prevalence of anti-UACA antibodies in Graves' disease was significantly higher than that in healthy controls (15% vs. 0%). Moreover, the prevalence of anti-UACA antibodies in Graves' ophthalmopathy was significantly higher than that in Graves' disease without ophthalmopathy (29% vs. 11%). We then investigated clinical manifestation of these patients with high UACA titer in detail. The prevalence of anti-UACA antibodies was 29% (9/31) in Graves' ophthalmopathy cases. These results clearly suggest that the appearance of anti-UACA antibody is strongly associated with eye muscle inflammation in patients with Graves' ophthalmopathy.

Thyroid-associated ophthalmopathy is considered to be an autoimmune disorder of eye muscle and surrounding orbital connective tissue and fat [3–7]. The eye symptoms associated with TAO can be classified into two subtypes, congestive ophthalmopathy (CO), in which inflammatory changes in periorbital tissues predominate, and ocular myopathy (OM), in which eye muscle is mainly damaged [30]. The current dogma tells that TAO is best explained by reactivity against thyroid and orbital tissue shared autoantigens [6,7]. One of such shared antigens is TSH receptor (TSHR), which is expressed in orbital preadipocytes. TSHR is mainly associated with the development of Graves' ophthalmopathy [8–11]. Several shared eye muscle and thyroid autoantigens have been investigated in eye muscle component in TAO, such as 63–67 kDa eye muscle membrane antigens and 55 kDa protein [12–24]. The flavoprotein (Fp) subunit of the mitochondrial enzyme succinate dehydrogenase is the so-called 64-kDa protein. Antibodies against Fp seem to be the best clinical marker of ophthalmopathy in patients with Graves' hyperthyroidism, and they are sensitive predictors for the development of eye muscle dysfunction in ophthalmopathy patients treated by antithyroid drugs [16,17]. The "55-kDa protein" was identified as G2s protein, eye muscle shared autoantigen with unknown function [22–24]. The primary reaction in eye muscle may be T-cell-mediated autoimmunity against TSHR of fibroblasts. The antibodies against Fp and G2s are produced secondary during the ophthalmopathy process, reflecting the release of sequestered cytoskeletal proteins from damaged eye muscles. Our observation indicates that UACA could be a novel candidate for thyroid and orbital shared autoantigen such as Fp in Graves' ophthalmopathy.

We also showed that UACA is expressed in eye muscle of patients with TAO as well as thyroid follicular cells in Graves' disease by immunohistochemical analysis. UACA was highly expressed in human eye muscle fibers of Graves' disease (Fig. 3D). This result indicates that UACA is simultaneously expressed in orbital eye muscle as well as thyroid follicular cells. High prevalence of anti-UACA antibodies is observed in patients with Graves' ophthalmopathy (Fig. 1). In particular, patients with severe ocular myopathy showed high UACA titer. Taken together, we presume that the appearance of anti-UACA antibodies could be a clinical marker for severe ocular myopathy, especially when its titer is high.

Wall and co-workers [16,17] suggested that anti-flavoprotein antibodies are produced by secondary immunoregulatory event resulting from eye muscle necrosis. They also showed that the prevalence of anti-G2s antibodies was 50% in Graves' ophthalmopathy, and anti-G2s antibodies appear in early phase of TAO [22–24]. In our study, the prevalence of anti-UACA antibodies in Graves' ophthalmopathy is lower (29%) compared with anti-G2s antibodies. If UACA is the primary autoantigen in Graves' ophthalmopathy, the prevalence should be higher. It is more likely that anti-UACA Ab is produced by secondary immunoregulatory process resulting from eye muscle necrosis like anti-flavoprotein antibodies. The low prevalence of anti-UACA Ab may raise the possibility that UACA is not relevant for the development of TAO. But, the prevalence of anti-UACA antibodies is only 20% in VKH disease, the original disease with anti-UACA antibodies. Because of the difficulty to produce recombinant UACA protein as a whole molecule (160 kDa), we used the C-terminal 18.0% portion of UACA to detect anti-UACA antibodies in patients' sera. A relatively lower prevalence of anti-UACA antibodies in Graves' patients may be due to the limited usage of C-terminal fragment of UACA protein for ELISA. To evaluate the presence of autoantibody against the whole UACA molecule, it is necessary to analyze patients' sera using other N-terminal fragments of UACA protein.

At present, the recognition of TSHR on the retro-ocular preadipocytes by TSHR autoantibodies and TSHR-specific T cells could be the initial event that drives the "homing" of the lymphocytes to the retro-orbital tissue. Then, the eye muscle inflammation is activated, resulting in the appearance of eye muscle autoantibodies including G2s, Fp, and UACA. Consequently, our observation about anti-UACA Ab is not contrary to this theory explaining the development of TAO. Since UACA is expressed in eye muscle, the appearance of anti-UACA antibodies may reflect immunological damage of eye muscle fiber, as observed in flavoprotein. We presume that not thyroid destruction but eye muscle destruction is directly associated with the production of anti-UACA antibody. If we examine more TAO cases with anti-UACA antibodies, we can identify the clinical relevance of anti-UACA antibodies for the development of TAO.

Although the physiological function of UACA protein is still unclear, UACA contains six ankyrin repeats and coiled coil domains, including a motif of leucine zipper pattern. Ankyrin repeat is 31–33 amino acid motif present in a number of proteins and contributing to protein–protein interactions [31]. In FRTL5 thyroid cells, the amount of UACA protein increased in a time- and dose-dependent manner following TSH stimulation. In the absence of TSH, UACA protein was diffusely distributed both in nucleus and cytoplasm of FRTL5 cells. Following TSH stimulation, UACA protein was exclusively recruited into nucleus of FRTL5 cell (Fig. 3A). Consequently, TSH augments UACA expression and simultaneously converts the localization of UACA within FRTL5 thyroid cells. Interestingly, UACA protein was highly expressed in nucleus of thyroid follicular cell in human thyroid tissue of Graves' disease. These results suggest that UACA protein may play a potential role for thyroid cell proliferation, since TSH drives the growth of thyroid follicular cells. Further study is necessary to reveal the physiological relevance of UACA in thyroid cell proliferation.

In summary, we demonstrate the high prevalence of anti-UACA autoantibodies in patients with Graves' disease. We confirmed that patients with Graves' ophthalmopathy (especially, with severe ocular myopathy) showed high UACA titer. UACA protein is expressed in autoimmune target tissues of Graves' disease, such as thyroid follicular cells and ocular eye muscles, indicating UACA is a novel thyroid–eye shared autoantigen. Although the sequence of autoantibodies production such as anti-G2s, anti-Fp or anti-UACA remains unknown, anti-UACA antibodies could be a clinical marker of ocular myopathy in patients with Graves' ophthalmopathy.

Acknowledgments

We appreciate Prof. Ito H (Division of Organ Pathology, Department of Microbiology and Pathology, Tottori University Faculty of Medicine, Yonago 683-8504, Japan) and Prof. Watanabe T (Division of Integrative physiology, Department of Functional, Morphological and Regulation Science, Tottori University Faculty of Medicine, Yonago 683-8504, Japan) for their kind technical advices and generous suggestions. We also appreciate TRANS GENIC INC. (Kumamoto 861-2202, Japan) for the production and kind supply of rabbit polyclonal anti-UACA antibodies.

References

[1] K. Yamada, S. Senju, T. Nakatsura, Y. Murata, M. Ishihara, S. Nakamura, S. Ohno, A. Negi, Y. Nishimura, Identification of a novel autoantigen UACA in patients with panuveitis, Biochem. Biophys. Res. Commun. 280 (2001) 1169–1176.
[2] F. Wilkin, V. Savonet, A. Radulescu, J. Petermans, J.E. Dumont, C. Maenhaut, Identification and characterization of novel genes modulated in the thyroid of dogs treated with methimazole and propylthiouracil, J. Biol. Chem. 271 (1996) 28451–28457.
[3] J. Kiljanski, V. Nebes, J.R. Wall, The ocular muscle cell is a target of the immune system in endocrine ophthalmopathy, Proc. Int. Arch. Allergy. Immunol. 106 (1995) 204–212.
[4] A.M. McGregor, Has the autoantigen for Graves' ophthalmopathy been found?, Lancet 352 (1998) 595–596.
[5] A.P. Weetman, Thyroid-associated eye disease: pathophysiology, Lancet 338 (1991) 28–35.

[6] J.R. Wall, M. Salvi, N. Bernard, A. Boucher, D. Haegert, Thyroid-associated ophthalmopathy-A model for the association of organ-specific autoimmune disorder, Immunol. Today 12 (1991) 150–153.
[7] H.B. Burch, L. Wartofsky, Graves' ophthalmopathy: current concepts regarding pathogenesis and management, Endocrinol. Rev. 14 (1993) 747–793.
[8] F. Karlsson, P. Dahlberg, P. Jansson, K. Westermark, P. Enoksson, Importance of TSH receptor activation in the development of severe endocrine ophthalmopathy, Acta Endocrinol. 121 (1989) 132–141.
[9] R.S. Bahn, C.M. Dutton, N. Natt, W. Joba, C. Spitzweg, E.A. Heufelder, Thyrotropin receptor expression in Graves' orbital adipose/connective tissues: potential autoantigen in Graves' ophthalmopathy, J. Clin. Endocrinol. Metab. 83 (1998) 998–1002.
[10] R. Paschke, A. Metcalfe, L. Alcalde, G. Vassart, A. Weetman, M. Ludgate, Presence of nonfunctional thyrotropin receptor variant transcripts in retroocular and other tissues, J. Clin. Endocrinol. Metab. 79 (1994) 1234–1238.
[11] R.S. Bahn, Pathophysiology of Graves' ophthalmopathy: the cycle of disease. J. Clin. Endocrinol. Metab. 88 (2003) 1939–1946.
[12] M. Salvi, A. Miller, J.R. Wall, Human orbital tissue and thyroid membranes express a 64kDa protein which is recognized by autoantibodies in the serum of patients with thyroid-associate ophthalmopathy, FEBS Lett. 232 (1988) 135–139.
[13] Y. Hiromatsu, M. Sato, K. Tanaka, S. Shoji, K. Nonaka, M. Chinami, H. Fukazawa, Significance of anti-eye muscle antibody in patients with thyroid-associated ophthalmopathy by quantitative Western blot, Autoimmunity 14 (1991) 1–8.
[14] Y-J. Wu, S.E.M. Clarke, P. Shepherd, Prevalence and significance of antibodies reactive with eye muscle membrane antigens in sera from patients with Graves' ophthalmopathy and other thyroid and nonthyroid disorders, Thyroid 8 (1998) 167–174.
[15] S. Kubota, K. Gunji, C. Stolarski, J.S. Kennerdell, J.R. Wall, Reevaluation of the prevalences of serum autoantibodies reactive with eye muscle antigens in patients with thyroid autoimmunity and ophthalmopathy, Thyroid 8 (1998) 175–179.
[16] S. Kubota, K. Gunji, B.A.C. Ackrell, B. Cochran, C. Stolarski, S. Wengrowicz, J.S. Kennerdell, Y. Hiromatsu, J. Wall, The 64-kDa eye muscle protein is the flavoprotein subunit of mitochondrial succinate dehydrogenase: the corresponding serum antibodies are good markers of an immune-medicated damage to the eye muscle in patients with Graves' hyperthyroidism, J. Clin. Endocrinol. Metab. 83 (1998) 433–447.
[17] K. Gunji, A. De Bellis, S. Kubota, J. Swanson, S. Wengrowicz, B. Cochran, B.A. Ackrell, M. Salvi, A. Bellastella, A. Bizzarro, A.A. Sinisi, J.R. Wall, Serum antibodies reactive against the flavoprotein subunit of succinate dehydrogenase are sensitive and specific markers of eye muscle autoimmunity in patients with Graves' hyperthyroidism, J. Clin. Endocrinol. Metab. 84 (1999) 16–22.
[18] Q. Dong, M. Ludgate, G. Vassart, Cloning and sequencing of a novel 64-kDa autoantigen recognized by patients with autoimmune thyroid disease, J. Clin. Endocrinol. Metab. 72 (1991) 1375–1381.
[19] A. Barsouk, S. Wengrowicz, D. Scalise, C. Stolarski, V. Nebes, M. Sato, J.R. Wall, New assays for the measurement of serum antibodies reactive with eye muscle membrane antigens confirm their significance in thyroid-associated ophthalmopathy, Thyroid 5 (1995) 195–200.
[20] T.C. Chang, T.J. Chang, Y.S. Huang, K.M. Hua, R.J. Su, S.C.S. Kao, Identification of autoantigen recognized by autoimmune ophthalmopathy sera with immunoblotting correlated with orbital computed tomography, Clin. Immunol. Immunopathol. 65 (1992) 161–166.
[21] M. Salvi, N. Bernard, A. Miller, Z.G. Zhang, E. Gardini, J.R. Wal, Prevalence of antibodies reactive with a 64kDa eye muscle membrane antigen in thyroid-associated ophthalmopathy, Thyroid 1 (1991) 207–213.
[22] K. Gunji, A. De Bellis, A.W. Li, M. Yamada, S. Kubota, B. Ackrell, S. Wengrowicz, A. Bellastella, A. Bizzarro, A. Sinisi, J.R. Wall, Cloning and characterization of the novel thyroid and eye muscle shared protein G2s: autoantibodies against G2s are closely associated with ophthalmopathy in patients with Graves' hyperthyroidism, J. Clin. Endocrinol. Metab. 85 (2000) 1641–1647.
[23] M. Yamada, A.W. Li, K.A. West, C.H. Chang, J.R. Wall, Experimental model for ophthalmopathy in BALB/c and outbred (CD-1) mice genetically immunized with G2s and the thyrotropin receptor, Autoimmunity 35 (2002) 403–413.
[24] A. De Bellis, A. Bizzarro, M. Conte, C. Coronella, S. Solimeno, S. Perrino, D. Sansone, M. Guaglione, J.R. Wall, A. Bellastella, Relationship between longitudinal behavior of some markers of eye autoimmunity and changes in ocular findings in patients with Graves' ophthalmopathy receiving corticosteroid therapy, Clin. Endocrinol. (Oxf.). 59 (2003) 388–395.
[25] K.C. Ossoinig, The role of standardized echography in Graves' disease, Acta Ophthalmol. (Copenh) 204 (1992) 81.
[26] X.P. Pang, J.M. Hershman, M. Chung, A.E. Pekary, Characterization of tumor necrosis factor-α receptors in human and rat thyroid cells and regulation of the receptors by thyrotropin, Endocrinology 125 (1989) 1783–1788.
[27] T. Ito, T. Seyama, T. Hayashi, K. Dohi, T. Mizuno, K. Iwamoto, N. Tsuyama, N. Nakamura, M. Akiyama, Establishment of two human thyroid carcinoma cell lines (8305C, 8505C) bearing p53 gene mutations, Int. J. Oncol. 4 (1994) 583–586.
[28] M. Derwahl, M. Kuemmel, P. Goretzki, H. Schatz, M. Broecker, Expression of the human TSH receptor in a human thyroid carcinoma cell line that lacks an endogenous TSH receptor, Biochem. Biophys. Res. Commun. 191 (1993) 1131–1138.
[29] J.A. Fagin, K. Matsuo, A. Karmakar, D.L. Chen, S.H. Tang, H.P. Koeffler, High prevalence of mutations of the p53 gene in poorly differentiated human thyroid carcinomas, J. Clin. Invest. 91 (1993) 179–184.
[30] T.P. Solovyeva, Endocrine ophthalmopathies. Problems of rational classification, Orbit 3 (1989) 193–198.
[31] S.E. Lux, K.M. John, V. Bennett, Analysis of cDNA for human erythrocyte ankyrin indicates a repeated structure with homology to tissue-differentiation and cell-cycle control proteins, Nature 344 (1990) 36–42.

Enhanced Priming of Antigen-Specific CTLs In Vivo by Embryonic Stem Cell-Derived Dendritic Cells Expressing Chemokine Along with Antigenic Protein: Application to Antitumor Vaccination[1]

Hidetake Matsuyoshi, Satoru Senju, Shinya Hirata, Yoshihiro Yoshitake, Yasushi Uemura, and Yasuharu Nishimura[2]

Dendritic cell (DC)-based immunotherapy is regarded as a promising means for anti-cancer therapy. The efficiency of T cell-priming in vivo by transferred DCs should depend on their encounter with T cells. In the present study, we attempted to improve the capacity of DCs to prime T cells in vivo by genetic modification to express chemokine with a T cell-attracting property. For genetic modification of DCs, we used a recently established method to generate DCs from mouse embryonic stem cells. We generated double-transfectant DCs expressing a chemokine along with a model Ag (OVA) by sequential transfection of embryonic stem cells, and then induced differentiation to DCs. We comparatively evaluated the effect of three kinds of chemokines; secondary lymphoid tissue chemokine (SLC), monokine induced by IFN-γ (Mig), and lymphotactin (Lptn). All three types of double transfectant DCs primed OVA-specific CTLs in vivo more efficiently than did DCs expressing only OVA, and the coexpression of SLC or Lptn was more effective than that of Mig. Immunization with DCs expressing OVA plus SLC or Mig provided protection from OVA-expressing tumor cells more potently than did immunization with OVA alone, and SLC was more effective than Mig. In contrast, coexpression of Lptn gave no additive effect on protection from the tumor. Collectively, among the three chemokines, expression of SLC was the most effective in enhancing antitumor immunity by transferred DCs in vivo. The findings provide useful information for the development of a potent DC-based cellular immunotherapy. *The Journal of Immunology,* **2004, 172: 776–786.**

Dendritic cells (DCs)[3] are potent immunostimulators. In vivo transfer of Ag-bearing DCs has proven efficient in priming T cell responses specific to Ag. DC-based methods are now regarded as being a promising approach for immunotherapy, especially for anti-cancer immunotherapy. DCs pulsed with peptide Ags or genetically modified to present Ags are currently being clinically tested in cases of immunotherapy for subjects with malignant tumors (1–4).

The efficiency of T cell-priming in vivo by injected DCs should depend on their encounter with T cells. When exogenous Ag was injected intracutaneously, ~25% of the DCs capturing the Ag migrated to the T cell area of draining lymph nodes (LN) (5), where they presented Ag to prime naive T cells specific to the Ag. In contrast, when bone marrow cell-derived DCs (BM-DCs) or splenic DCs are transferred exogenously by s.c. or i.p. injection, the absolute number of the DCs found within the draining LN represented only a small proportion (0.1–1%) (6–8). It has also been reported that almost all of transferred DCs remained at the s.c. immunization site 24 h after transfer (9). Inefficient migration of exogenous DCs to lymphoid organs may lower the frequency of their encounter with T cells. Therefore, it may be possible to improve the efficacy of exogenously transferred DCs to prime immune responses by augmenting their encounter with T cells. For example, if transferred DCs produce chemokines to intensively attract T cells, they may prime immune response efficiently, even though the DCs do not migrate to lymphoid organs.

Several kinds of chemokines with the capacity to attract T cells are produced by different cell types. Secondary lymphoid tissue chemokine (SLC)/CCL21 is produced in T cell regions of LN and spleen and also by high endothelial venules in LN. SLC chemoattracts T cells, NK cells, B cells, and DCs (10–12). Monokine induced by IFN-γ (Mig)/CXCL9 is produced by macrophages and binds to the chemokine receptor CXCR3, which mediates the recruitment of predominantly Th1 cells and activated NK cells (13). Lymphotactin (Lptn)/XCL1, produced by activated T cells, has chemoattractive properties on $CD4^+$ and $CD8^+$ T cells and on NK cells (14, 15). This chemotactic action of Lptn is mediated through the receptor XCR1.

Recently, we established a novel method for genetic modification of DCs, where we generated DCs from mouse embryonic stem (ES) cells by in vitro differentiation (16). ES cell-derived DCs (ES-DCs) express MHC class II, CD11c, CD80, and CD86. They can strongly simulate MLR and efficiently process and present protein Ag to T cells. Their capacity to do so is comparable to that of BM-DCs. We can readily generate genetically modified DCs by introducing expression vectors driven by a β-actin promoter and subsequent

Department of Immunogenetics, Graduate School of Medical Sciences, Kumamoto University, Kumamoto, Japan

Received for publication April 29, 2003. Accepted for publication September 30, 2003.

The costs of publication of this article were defrayed in part by the payment of page charges. This article must therefore be hereby marked *advertisement* in accordance with 18 U.S.C. Section 1734 solely to indicate this fact.

[1] This work was supported in part by Grants-in-Aid 14657082, 14570421, 14370115, and 12213111 from the Ministry of Education, Science, Technology, Sports, and Culture, Japan, and a research grant for Intractable Diseases from the Ministry of Health and Welfare, Japan.

[2] Address correspondence and reprint requests to Dr. Yasuharu Nishimura, Department of Immunogenetics, Graduate School of Medical Sciences, Kumamoto University, Honjo 1-1-1, Kumamoto 860-8556, Japan. E-mail address: mxnishim@gpo.kumamoto-u.ac.jp

[3] Abbreviations used in this paper: DC, dendritic cell; ES, embryonic stem cell; SLC, secondary lymphoid tissue chemokine; Mig, monokine induced by IFN-γ; Lptn, lymphotactin; LN, lymph node; BM-DC, bone marrow cell-derived DC; ES-DC, ES cell-derived DC; neo-R, neomycin resistant; IRES, internal ribosomal entry site.

0022-1767/04/$02.00